UNIVERSIDAD DE SANTIAGO DE CHILE

FACULTAD DE CIENCIA

Departamento de Física

QED at the limit: Dark Matter and Strong Fields.

Natalia Angélica Tapia Arellano

Profesores Guía:

Jorge Gamboa Ríos

Fernando Méndez

Tesis para optar al grado de Doctor en Ciencia con Mención en Física.

Santiago – Chile

2019

QED at the limit: Dark Matter and Strong Fields

Natalia Angélica Tapia Arellano

Este trabajo de titulación fue preparado bajo la supervisión del (los) profesor(es) guía Dr. Jorge Gamboa y Dr. Fernando Méndez del Departamento de Física y ha sido aprobado por los siguientes miembros de la comisión calificadora del candidato:

.....

Dr. Jorge Alfaro

.....

Dr. Dora Altbir

.....

Dr. Paola Arias

.....

Dr. Jorge Gamboa

.....

Dr. Fernando Mendez

.....

Dr. Mikhail Plyushchay

.....

Dr. Roberto Bernal

Director Departamento de Física

Facultad de Ciencia

Resumen

En esta tesis se muestran en detalle dos problemas que fueron parte de este trabajo de doctorado. El primer proyecto está relacionado con calcular las contribuciones de distintos procesos a la corrección del momento magnético de un fotón Dark [15]. Para esto se consideró un modelo de electrodinámica cuántica Dark, acoplada a un fotón visible, por medio de un término de kinetic mixing. La contribución principal es la correción del vértice que contiene fotones y fermiones dark. Al siguiente orden en términos del parámetro de kinetic mixing η, también se calcula la corrección de un vértice con un fotón externo visible. Se discute la relación entre ambas contribuciones. El factor giromagnético del fermión dark es determinado en términos de las cotas de masas para el fotón y el fermión dark. Finalmente se obtiene una expresión para los factores giromagnéticos de los dos procesos considerados, en términos de la razón de masas entre el fotón dark y el fermión dark. Cuando el comportamiento es similar a QED, es decir cuando la masa del fotón dark es muy pequeña en comparación a la del fermión dark (como ocurre en QED), se recupera el comportamiento de la materia visible.

En el segundo capítulo de esta tesis, se presentan los resultados para las

tasas de creación de pares electrón-positrón, que se espera sean medidas en el experimento LUXE en DESY, Hamburgo [34]. En este experimento se espera obtener un espectro de Bremsstrahlung, haciendo chocar el haz de electrones de 17.5 GeV con una lámina delgada (foil) y se guiará a los resultantes fotones para colisionar con un láser de alta intensidad, de alrededor de $10^{20} W/cm^2$. Se espera que esta intensidad alcance rangos cercanos al límite no perturbativo en el cual creación espontánea de pares electrón-positrón sería observada. El régimen no-pertubativo estaría representado en este caso por una intensidad por sobre los $5 \times 10^{18} W/cm^2$ y se espera observar pares a partir de $3 \times 10^{18} W/cm^2$. Esta medición permitiría una verificación indirecta del campo crítico de la electrodinámica cuántica predicho por Sauter en 1931.

Palabras clave: Momento magnético anómalo, Materia Oscura, Kinetic Mixing, QED dark, Factor giromagnético, Campos fuertes, Límite de Schwinger, Régimen no perturbativo, Campo crítco de la QED.

Abstract

In this thesis it is shown in details two problems which were part of this PhD work. The first project is related to compute the different processes contributions to the Dark photon magnetic moment correction [15]. For this a Dark QED has been considered, coupled to a visible photon, by means of a kinetic mixing. The most important contribution comes from the corresponding vertex, is that one in which only dark matter plays a role with dark photons and fermions. The next leading contributions are given by a visible external photon vertex, being each next order contribution less important. We have found a relation between both contributions, given by the kinetic mixing parameter η. The gyromagnetic factor of the dark fermion is determined in terms of the masses expected for the dark photon and fermion. When the behaviour is similar to QED, that is, when the mass of the dark photon is very small compared to that of the dark fermion one (as in QED), the behaviour of visible matter is recovered.

The second chapter in this thesis, presents the results for the electron positron pair production rates, expected to be measured at LUXE experiment in DESY [34], Hamburg. In this experiment a Bremsstrahlung spec-

trum will be obtained by colliding an electron beam of 17.5 GeV with a thin foil and the high energy photons obtained will be lead into collision with a high intensity laser beam, around $10^{20}W/cm^2$. It is expected for this intensity to reach a range near the non perturbative limit in where spontaneous pair production of electrons and positrons is expected. The non-perturbative regime would be represented in this case by an intensity above $5\times10^{18}W/cm^2$ and it is expected to observe pairs from $3 \times 10^{18}W/cm^2$.The measurement of this rate would allow an indirect verification of the critical electric field, predicted by Sauter in 1931.

Keywords: Anomalous magnetic moment, Dark Matter, Kinetic Mixing, Dark-QED, Gyromagnetic factor, Strong fields, Schwinger limit, Non-perturbative regime, QED critical field.

Acknowledgements

I would like to thank my thesis supervisor, Professor Jorge Gamboa, who supported me and believed in me, even before I had started the PhD program, and also in times when I didn't trusted myself. I would like to thank Professor Fernando Mendez and Professor Paola Arias, who actively contributed to my formation as a physicist. To Professor Dora Altbir and Eugenio Hamm, to the University of Santiago Physics Department, and to the Physics PhD program secretaries. To University of Santiago and Conicyt national scholarship 21160064.

I also thank to Professor Andreas Ringwald, with whom I worked during 10 months at the Deutsches Elektronen-Synchrotron (DESY), also to Professor Manu Paranjape for 6 months of collaboration at Université de Montréal.

Agradecimientos

Por sobre todo quisiera agradecer a mi Profesor guía, el Profesor Jorge Gamboa, quien incluso antes de comenzar el programa de Doctorado, me apoyó incondicionalmente y creyó en mí incluso cuando yo misma no me sentí capaz. Agradezco al profesor Fernando Méndez y a la profesora Paola Arias quienes contribuyeron de forma activa en mi formación. A la profesora Dora Altbir y al profesor Eugenio Hamm, al Departamento de Física de la Universidad de Santiago de Chile, a las secretarias del programa de Doctorado en Ciencias con mención en Física. A la Universidad de Santiago de Chile y la beca Conicyt Doctorado Nacional 21160064.

Agradezco también al Profesor Andreas Ringwald con quien trabajé durante 10 meses en el Deutsches Elektronen-Synchrotron (DESY), también al Profesor Manu Paranjape por 6 meses de colaboración en la Université de Montréal.

Agradezco a mi familia completa. Personalmente a Jorge Arellano Navarro, quien me enseñó a contar y que siempre me dijo que estudiar era lo más maravilloso del mundo. A Daniel Tapia Arellano, por su confianza y fe en mí. A Eduardo Curín Mayorga, por estar siempre ahí. A Lorena y Fernando

Tapia.

Finalmente agradezco a Liliana Arellano Castelar, mi madre. Por cada día de trabajo, cada esfuerzo, cada desaliento, cada momento en el que el sacrificio fue más allá. En este trabajo está tu sangre, sudor y lágrimas y cada página va dedicada a ti.

Contents

List of Tables

List of Figures

Introduction

At the very beginning, the primordial matter was extremely dense, compressed and hot, just after the Big-Bang, which is the assumption of a huge explosion and the most accepted theory for the origin of the universe. Only elementary particles composed the matter at that time, known today as quarks and leptons. The primordial matter expanded and in this process it cooled down, quarks formed heavier particles, hadrons and these were of two kinds, baryons or mesons, with three and two quarks (a quark and an antiquark) respectively. The electrons were captured by nuclei, formed by protons and neutrons which are baryons and in this way giving place to the first atoms.

Large amounts of primordial matter started to collect and form stars, and larger and heavier nuclei were formed inside of them. When the stars had enough matter, some of their mass was ejected to the interestelar space, helping in the creation of new stars, planets and other interesting objects in the universe. The union of atoms in molecules created chemical substances giving birth to complex structures.

Cosmology and astrophysics study the evolution of the universe; the syn-

thesis of heavy nuclei from lighter ones for conditions inside stars is the object of study of nuclear astrophysics. Nuclear physics studies the behaviour of nuclei under normal conditions or in excited states, as well as the reactions among them. The structure of atomic molecules and their reactions is what chemistry searches. Finally, biology studies the formation and developments of the great agglomerates that compose life. All of these sciences have as an objective the understanding of complex structures starting from simpler ones and their interactions between them [8].

Quantum field theory (QFT) provides an extremely powerful set of computational methods that has led to important agreement between theoretical predictions and experimental data in the history of science. QFT is primarily a theory of physics, not mathematics which dispenses a set of tools in order to perform practical calculations, calculations that can predict, sometimes with incredibly accuracy, numbers that can be measured in experiments. Finally QFT is the basic mathematical language that is used in order to describe and analyse the physics of elementary particles. It is the theory of creation and destruction of particles, due to the famous equation $E = mc^2$, the confluence between special relativity and quantum mechanics.

Quantum electrodynamics (QED) speaks for the merger of three great concepts: classical electrodynamics (Maxwell's theory), quantum mechanics and special relativity. It was completed by 1930 with contributions from several actors; it combined the electron's Dirac theory and the quantization of the electromagnetic field into individual photons. The problem with divergences and renormalization and its handling includes the input made

by Bethe, Feynman, Tomonaga, Schwinger, Dyson and others. After this, QED was tested to incredible precision. In order to test the theory, higher order (loops) effects in perturbation theory must be considered, due to the precision of these tests and because some effects, as light by light scattering, can only be observed over four order and loop level.

Having the above information in mind, QED is the most successful theory in physics when judged in terms of the precision of its experimental tests and theory.

Some tests of QED include the Lamb shift, muonium (μ^+e^- bound states), positronium (e^+e^- bound states) and physical constants as α, the fine structure constant and which represents a good measure of the strength of the electromagnetic force [31]. For this last one, the most precise measurement comes from the anomalous magnetic moment of the electron [42], computed by Schwinger in 1948, which enable us to test higher order corrections. The precision of both the theoretical and experimental results tell us about the validity of Quantum Electrodynamics.

In this thesis we will deal with phenomena that occur in the presence of a strong electromagnetic field. An effect which cannot be described in terms of perturbation theory will occur under these circumstances. The ground state of the theory, the vacuum of QED will become unstable at a certain strength of the potential.

Usually in QED the lowest energy state (the vacuum), is characterised by the fact that no particles, electrons and positrons are present: all positive energy states are empty and all negative energy states are occupied. The

physically observable vacuum of the theory, without and electromagnetic field, is free and neutral.

Now we consider some field A_μ is switched on, a classical electromagnetic field, not influenced by electrons, this can be considered as an atomic nucleus, with charge $-Ze$. Remembering Einstein's famous $E = mc^2$, if we have a potential so strong it will surpass the barrier by adding one electron to the system and the effect it will suffer is that the system will feel lighter than it would be without this new electron [32]. However it is not possible to have one single electron, only electron-positron pairs can be produced, which has a threshold energy of $2mc^2$. These pairs can be separated spatially by the corresponding strong electric field by expenditure of this threshold energy.

If we go beyond a critical potential strength pairs of e^+e^- will be created spontaneously and the vacuum will decay into a charged vacuum.

If we make a rough estimation we will get that this pair production will become considerable if the potential $\Delta V = e\Delta A$ changes by the value of the rest mass of the electron mc^2 over a characteristic length scale, set by the Compton wavelength of the electron $\lambda = \hbar/mc$. The electric field is given by $E = -\nabla A$, so we will get a critical electric field associated to the critical potential, being $E_{crit} = 1.3 \times 10^{18} V/m$ [1]. The QED critical field can be translated in terms of intensity for an experimental set-up, being of $\sim 10^{29} W/cm^2$.

It is of fundamental interest to observe nonlinear quantum effects, spe-

[1] $E_{crit} \sim \frac{\Delta A}{\Delta x} = \frac{mc^2}{e\hbar/mc} = \frac{m^2c^3}{e\hbar} = \frac{1}{e}\frac{511keV}{386fm} = 1.3 \times 10^{18} V/m$

cially from the point of view of the validity of QED for fields near the critical field. In spite of the impossibility to create such an intense field in a laboratory, it is possible to reach an intensity in the rest frame of the particle of order of the critical field, from its point of view. The study of nonlinear quantum effects due to interaction of elementary particles with the field of a plane electromagnetic field it is important and interesting and is one of the subjects of this thesis.

The discovery of the Higgs particle closes around 40 years of verifying the Standard Model (SM), however, there are notorious problems still unresolved about it. The fine-tuning hierarchy problems between weak interactions and gravity scales is maybe the most pressing one. Observations of matter in the Earth, other planets in the Solar System or beyond, stars or galaxies, suggest matter and anti-matter asymmetry, related to CP violation and which amount accounted from SM is not enough to explain the evolution of the universe from a symmetric configuration to a matter-dominated Universe as we know it. There is no evidence for new TEV-scale physics as could be supersymmetry, one of the many ideas proposed to explain or at least stabilise the problem of hierarchy. Dark energy and dark matter add another mystery to the puzzle, besides all the experimental efforts to identify the nature of the last one, inferred from its gravitational effects, that has led to any concluding result, excluding most of the parameter space for supersymmetric dark matter. In spite of being successful, Standard Model is a complicated theory and for this and other reasons, a search beyond the SM has started.

Evidence has been accumulated through the last century in relation with

the existence of Dark Matter (DM). Either from galactic rotation curves, the motion of galaxies in clusters, gravitational lensing or the cosmic microwave radiation (CMB) we know that there is much more matter in the Universe corresponding to luminous matter; stars, gas and other forms of it [42]. This "missing matter"does not seem to be baryonic matter, i.e. Standard Model matter, that is somehow hidden. Baryonic matter is determined by Big Bang Nucleosynthesis (BBN) and CMB. This "new"(dark) matter presumably must interact at most weakly with electromagnetism.

One possibility in order to explain this phenomena related to Dark Matter is primordial black holes (PBH), formed somehow prior to BBN. Considering the astrophysical constraints on the density of PBHs, there is a window on which they constitute dark matter, or at least a fraction of it.

Dark Matter is usually associated with elementary particles, whose candidates are commonly classified as hot, warm or cold depending on whether they were relativistic, intermediate or non-relativistic when they decoupled from equilibrium in the early universe. Hot dark matter (light massive neutrinos for example) is excluded, basically because, on small scales it does not cluster sufficiently. On the other hand, a viable candidate for warm dark matter is keV-scale sterile neutrinos.

Most likely scenario for cold dark matter (CDM) involves a stable, on cosmological time scales, neutral colorless particle "χ", ussually with spin 0 or 1/2 and which may or may not be different from its antiparticle $\bar{\chi}$. If weakly interacting massive particles (WIMPs) are considered, it leads to dark matter densities, known as the WIMP miracle. WIMP candidates can

be the lightest supersymmetric partner (neutralino, usually), or analogous stable particles in Little Higgs or universal extra dimension models. However, the parameter space allowed for these conventional candidates is being reduced due to experimental constraints, which gives a motivation to think of much lighter dark matter candidates with very weakly coupling to ordinary particles. Approaching like these, may be connected to the ordinary visible sector by a kinetic mixing of the Z with a new Z' gauge boson, or other types of portals with Higgs bosons, neutrinos, axions, etc.

There are several experimental searches on WIMPs and similar particles in a direct, indirect and collider fashion. Direct search experiments look for the nuclear recoil of an elastic or possible inelastic scattering $\chi N \to \chi N$.

Indirect detection searches refers to the results coming from the annihilation or possible decays of dark matter particles into gamma rays, neutrinos, positrons, etc., in regions of high concentration, also from the decays or secondary interactions of particles that were produced from dark matter. Signals near the galactic center might be related to the direct annihilation into mono-energetic photons, or continuum photons, or antiparticles from secondary processes.

In spite of the various signal hints detected of photons or excess of antiparticles, none of them have proven to be compelling due to possible astrophysical backgrounds.

Dark Matter particles have been searched at ATLAS and CMS [42] in a signal with particle "X" and a large missing transverse momentum, so far, no positive signals have been observed.

Having in mind the precision tests of QED and Dark Matter searches we also take into consideration the information published about the Fermi-LAT data on the cosmic gamma-ray spectrum from the Galactic center. Such high energy photons can be induced by a dark matter annihilation or decay.

Being a tremendous milestone in QED success, the anomalous magnetic moment can play an important role also in Dark Matter and it can be considered to have something to do with the luminosity excess in the center of the galaxy (see [33]). The direct detection of dark matter with a magnetic moment could be realized in a variety of ways and possibilities have been proposed here [28].

In this thesis we present, two different problems which can be labeled under the field of Quantum Electrodynamics, for visible and Dark Matter. Every problem will be explained in a different chapter with its own introduction and development.

The objectives of the present thesis are, for each chapter are:

1. The first problem is Dark Matter and Kinetic Mixing. We presente a Dark Quantum Electrodynamics in which a dark fermion is coupled to the visible photon. The objective is to compute the correction to the dark fermion magnetic moment. For this it is studied two possible vertex contributions, the first one considering only dark matter, in which the loop and external photon are dark and that will not be perceptible, and another contribution coming from a dark photon in the loop and a visible external photon. This last one would be the

leading visible contribution.

2. In the second chapter, we show results for electron positron pair production in strong field petawatt lasers in where it is expected, for non-perturbative pair production near the Schwinger limit, to be observed. The aim is to compute the rate of electron-positron pair production as expected for the next experiment to be perform at DESY, the LUXE experiment, in which a 17.5 GeV electron beam will be brought into collision with a foil (a thin sheet), in order to obtain Bremsstrahlung high energy photons. These high energy photons will be lead to collision again with a High Intensity petawatt laser and pair production near the Schwinger non perturbative limit will take place.

In this thesis also, it has been have added a brief discussion about stability in negative mass bubbles. It is thought that regions of negative energy density in the Universe can undergo gravitational collapse into a black hole [45]. There are also some ideas about a "dark fluid"of negative mass theory containing dark matter and dark energy in it [26]. What we have considered in this case for the solutions to Einstein equations by a spherical geometry, found by Schwarzschild, a negative mass black hole. It was found that this is possible to have a stable configuration for a negative bubble mass and it was taken into consideration, dominant energy conditions to be fulfilled. The results related to this work can be found in Appendix A.

Finally it was added as Appendix B, the articles mentioned in this thesis [2, 4], which have not been discussed in detail but that were also part of the

work developed during the PhD.

Chapter 1

Dark Matter and Kinetic Mixing: Anomalous $g-2$

1.1 Introduction

The standard model, which is the most successful theory at the moment to help us understand the universe around us, is an incomplete theory. This is why it is necessary to go beyond. Since the 70's there is enough evidence confirming the existence of Dark Matter, but until now there is no evidence that would confirm its participation in processes that we could measure. The first indicator of physics beyond standard model can be found in the neutrino masses. These particles suffer oscillations, which are only possible if they have mass, a mass which is not considered in the standard model, due to breaking of symmetry. These particles were the first candidates of dark matter, but this idea was ruled out for the three neutrinos known (electronic, muonic and tau neutrino). There is some chance of the existence of a fourth

neutrino, sterile, interacting in an imperceptible way with ordinary matter, which would be a candidate for dark matter, but the expected densities do not correspond with the amount of dark matter known to exists (five times more abundant than normal matter). It is necessary to continue this search in order to understand our universe origin and its future, in accordance with the predictions that we can make under our understanding.

In this section of the thesis we present the result of the research during the second year of PhD formation, in which it was worked in two projects [15, 4] with Professor Jorge Gamboa at University of Santiago de Chile. For the first project it was considered a model of dark quantum electrodynamics (QEDs) coupled to a visible photon through a kinetic mixing term. The $g_\Psi - 2$ for the dark fermion was computed, where g_Ψ is its gyromagnetic factor. Here, a relation between the gyromagnetic factor related to the dark matter process and the visible process through a constant was found, which depends on the kinetic mixing factor. On the last project, which will not be detailed in this thesis (see [4]), it was computed the analogous of the light-by-light diagram from two dark photons to a visible pair of standard model particles and an expression for the differential cross section. For high energy beams, this differential cross section could be measurable with a magnitude similar to the neutrino cross section.

1.2 Dark Matter anomalous magnetic moment

How can we connect dark matter physics and the visible sector of the Universe? Until now we only know that Dark Matter interacts very weakly with visible matter (see [30] and [43]). Maybe the most appropriate way to detect it is by indirect ways, like dark matter-antimatter annihilation for example, which could be an answer to the visible energy and matter over-abundance in the center of galaxies [25].

If dark matter exists in a particle form, it has to be in particles whose description is beyond the Standard Model. No particle in the Standard Model can play the role of a Dark Matter particle. The easiest example for this idea are WIMP particles, which should have been created at the early universe and have some probability to annihilate into Standard Model particles, at the Sun or in the center of the galaxy [1].

A Standard Model minimal extension can be obtained by adding a new U(1) gauge symmetry which is spontaneously broken, giving mass to the dark photon [40].

But what about the question at the beginning of this section, in how to

[1] Also in the literature WISP's are discussed (weak interacting slight particles) which is a distinction for the light sector of dark matter, nonetheless if dark matters is completely understood, WIMP's and WISP's would be contained in just one formalism and because of that is that in this case the word used will be WIMP without making the distinction on the mass.

connect dark matter and visible sector: this is done by means of a ***kinetic mixing***. In this way dark and visible sector are bounded because it is possible to have a small kinetic mixing term between a dark photon and the Standard Model. Dark Matter particles can be trapped at the Sun in interactions with nuclei or electrons, thermalising the interior of the Sun and interacting with other Dark Matter particles, annihilating to particles as neutrinos for example. This can be translated into detectable signals on Earth [40].

Our dark matter candidate interacts through a dark U(1) gauge symmetry. The kinetic mixing terms can rise from the interaction between a massive charged particle in the electromagnetic and dark electromagnetic group [40].

A scheme that could give new ideas about the luminosity excess at galaxies center is that one from a non-Abelian dark sector with admisible stable solutions, topologically classical and massive; weakly interacting charged monopoles created at the beginning of the universe at a very energetic event. It could happen the annihilation of a monopole and anti-monopole giving place to a non-topological energy emitting particle like object, dark and visible ones. If these monopoles are very massive, they can be gravitationally attracted by galaxies that enhances the probability for this annihilation to occur in their neighbourhood.

Kinetic mixing mechanism requires interaction between visible photons (A_μ) and dark photons (B_μ), interaction which can be implemented diversely, one way can be found in a detailed form in [27], where the kinetic mixing

term is written as follows

$$\eta F_{\mu\nu}(A)F^{\mu\nu}(B) \equiv \eta F(A)F(B), \tag{1.1}$$

η is the kinetic mixing parameter, considered to be very small.

These fields in the following theory interact with dark matter as

$$\mathcal{L} = \bar{\Psi}\left(i\partial\!\!\!/ - B\!\!\!/ - m_\Psi\right)\Psi - \frac{1}{4}F^2(B) - \frac{1}{4}F^2(A) + \frac{\eta}{2}F(A)F(B), \tag{1.2}$$

in which it has been taken $e = 1$.

For eq. (1.2), Ψ is a dark fermionic massive field with charge 1, B_μ corresponds to the dark photon ($\gamma^\mu B_\mu = B\!\!\!/$), A_μ is the visible photon field and the dark fermion mass is represented by m_Ψ.

It is convenient to write eq. (1.2) as

$$\mathcal{L} = \mathcal{L}_{dark-fermion} + \mathcal{L}(A, B), \tag{1.3}$$

where

$$\mathcal{L}(A, B) = -\frac{1}{4}F^2(A) - \frac{1}{4}F^2(B) + \frac{\eta}{2}F(A)F(B), \tag{1.4}$$

which can diagonalised by means of the following transformation $B'_\mu = B_\mu - \eta A_\mu$, and obtaining

$$\mathcal{L}(A, B') = -\frac{1-\eta 2}{4}F^2(A) - \frac{1}{4}F^2(B') = -\frac{1}{4e^2_{(-)}}F^2(A) - \frac{1}{4}F^2(B'), \tag{1.5}$$

thus it is obtained for eq. (1.2)

$$\mathcal{L} = \bar{\Psi}\left(i\partial\!\!\!/ - B\!\!\!/' - \eta A\!\!\!/ - m_{\Psi}\right)\Psi - \frac{1}{4e_{(-)}^2}F^2(A) - \frac{1}{4}F^2(B'). \tag{1.6}$$

It can be observed in this last expression which is now diagonalized the effect of this diagonalization, electric charge renormalization

$$e_{(-)} = \frac{1}{\sqrt{1-\eta^2}}. \tag{1.7}$$

It is nice to notice that the diagonalization has a physical effect in the visible gauge field, actually, we observe that the visible photons now couple to the dark fermion through the "millicharge" η, this means only a small fraction of the visible charge perceives the dark fermion, as a consequence of a very small kinetic mixing [2] ([1],[11], [12]).

Another result from diagonalization will be a change in the interaction terms. Before performing the diagonalization, the interaction term had the form $\bar{\Psi}\gamma^{\mu}\Psi B_{\mu}$, which means dark sector QED as can be seen to first and second order in Figure 1.2. After diagonalizing, the interaction term changes to $\bar{\Psi}\gamma^{\mu}\Psi(B'_{\mu} - \eta A_{\mu})$. The kinetic mixing term allows for a dark QED process with dark fermions to produce visible photons (see Figure 1.1). Some of this processes are very interesting from the physical point of view, in the case of annihilation of dark matter it can give place to visible photons and also in other processes which are a consequence from kinetic mixing [3].

[2] For an alternative kinetic mixing term, different from (eq. (1.1)), see [27].

[3] Some of this processes could give a hint about an unsolved problem related to the galaxy

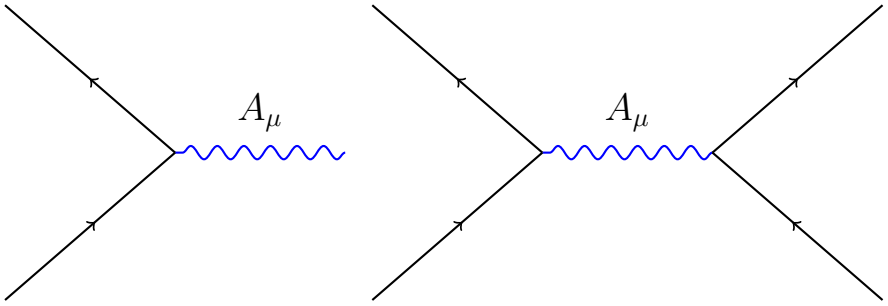

(a) First order interaction (b) Second order interaction

Figure 1.1: QED Diagrams. Visible photon fields A_μ are shown in blue. This is the result of a diagonalization in the Lagrangian including a Dark-QED and a visible photon. After this process now we can have interaction between visible and Dark Matter.

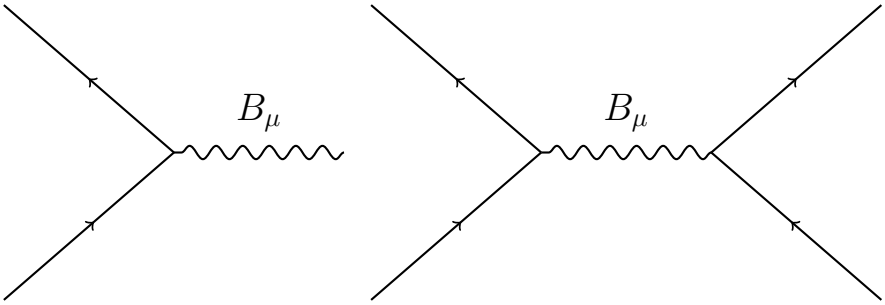

(a) First order interaction (b) Second order interaction

Figure 1.2: Dark QED Diagrams. Interactions between Dark Matter only.

What if the interaction or the scattering process between a nucleus and a dark matter particle is electromagnetic intrinsically? This interaction could happen by means of the dark matter dipolar magnetic moment, which can be induced by the short range physics underlying at the first or next loop. Dipolar magnetic moment have a dominant contribution to DM-nucleus scattering due to the direct coupling with nuclear charge.

center excess of luminosity [21].

The electron has an anomalous magnetic moment, which has a small contribution in the electron scattering correction at one loop for the vertex function itself, that arises from and additional photon ([55],[59]).

From where does this correction come from? It is well known in quantum electrodynamics, but here is briefly discussed. Dirac equation in the non-relativistic limit couples to and external magnetic field through the Hamiltonian:

$$H = \frac{\vec{p}}{2m} + V(r) + \frac{e}{2m}\vec{B} \cdot (\vec{L} + g\vec{S}). \tag{1.8}$$

In this last expression g represents the relative force of its dipolar magnetic moment to the spin-orbit coupling strength. Dirac equation implies $g = 2$ but there are also quantum corrections. Starting from Dirac equation, charged spinors satisfy:

$$(i\not{D} - m)\Psi = 0, \tag{1.9}$$

in which $\not{D} = \not{\partial} + ie\not{A}$. It is easy to see that spinors also satisfy

$$(\not{D}^2 + m^2)\Psi = 0, \tag{1.10}$$

when $(i\not{D} + m)$ is multiplied.

A bit of algebra shows that

$$\not{D}^2 = D_\mu^2 + \frac{e}{2}F_{\mu\nu}\sigma^{\mu\nu}, \tag{1.11}$$

and thus

$$(D_\mu^2 + \frac{e}{2}F_{\mu\nu}\sigma^{\mu\nu} + m^2)\Psi = 0, \tag{1.12}$$

to finally obtain

$$\frac{(H - eA_0)^2}{2m}\Psi = \left(\frac{m}{2} + \frac{(\vec{p}^2 - e\vec{A})^2}{2m} - 2\frac{e}{2m}\vec{B}\cdot\vec{S} \pm i\frac{e}{m}\vec{E}\cdot\vec{S}\right)\Psi. \tag{1.13}$$

The term $\frac{e}{2}F_{\mu\nu}\sigma^{\mu\nu}$ makes the difference with the scalar field, that satisfies $(D_\mu^2 + m^2)\Phi = 0$. To look for corrections in g we have to search in the S matrix for loops with the same effect as a term $\sigma_{\mu\nu}F^{\mu\nu}$ in the Lagrangian. This corrections have the shape in which photons interact with fermions

The sum of all the corrections to this vertex are called Γ^μ and represents corrections to the answer of an electron to an external magnetic field. The process itself is $e^-(q)A_\mu \to e^-(q')$, with two spinor states $\bar{u}(q')$ y $u(q)$ and polarisation vector $\epsilon_\mu(p)$,

$i\mathcal{M}^\mu =$ 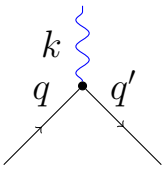

$= i\,\eta\,\bar{u}(q')\gamma^\mu u(q),$ (1.14)

the photon moment has the following restriction $k^\mu = q'^\mu - q^\mu$.

The vertex correction modifies the previous assessment and the vertex function will be modified in the next way

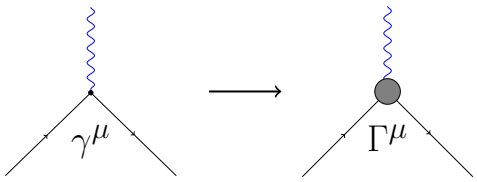

so now we will have for the vertex function to be:

$$\begin{aligned} i\mathcal{M}'^{\mu} &= (-i\eta)\bar{u}(q')\,\Gamma^{\mu}\,u(q) \\ &= (-i\eta)\bar{u}(q')\left[F_1\left(\frac{k^2}{m_\Psi^2}\right)\gamma^\mu + \frac{i\sigma^{\mu\nu}}{2m_\Psi}k_\nu F_2\left(\frac{k^2}{m_\Psi^2}\right)\right]u(q), \quad (1.15) \end{aligned}$$

in which F_1 and F_2 are form factors and $\Gamma^\mu = \left[F_1\left(\frac{k^2}{m_\Psi^2}\right)\gamma^\mu + \frac{i\sigma^{\mu\nu}}{2m_\Psi}k_\nu F_2\left(\frac{k^2}{m_\Psi^2}\right)\right]$.

F_1 form factor is related to electric charge corrections instead of anomalous magnetic moment as in F_2 case.

One loop diagram as in Figure 1.3(a) and 1.3(b) are photon and fermion propagator corrections, respectively. Later it will be clearer why just one of the four processes which could contribute to the vertex (1.14), contributes to the vertex correction in spite of the other contributions, which only contribute to propagator corrections. In the diagram below it can be seen corrections up to third order with dark fermion interactions and one visible photon

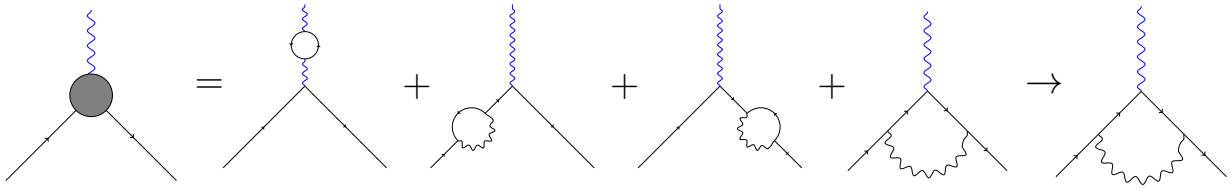

in which only the last term has contributions to the magnetic moment.

For this diagram we have

$$i\mathcal{M}'^{\mu} = \qquad (1.16)$$

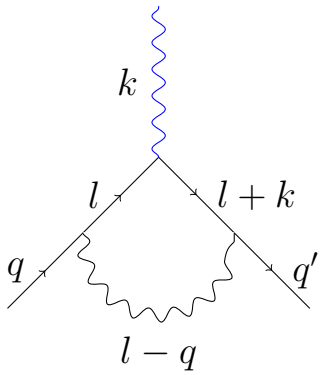

It is customary to remember the kind of interactions in QED and which one of them would have a variation due to kinetic mixing term.

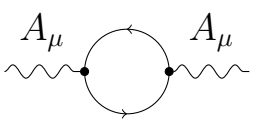

(a) Vacuum polarization or photon self energy

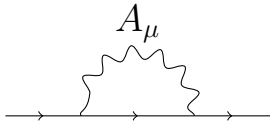

(b) Electron self energy

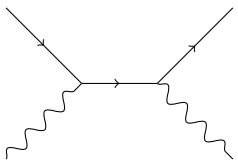

(c) Compton Scattering

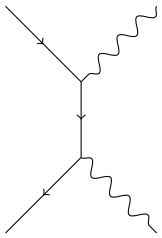

(d) Pair annihilation

Figure 1.3: Second order QED diagrams. For Dark QED we have the same interactions but with dark photons B_μ (in this case the field A_ν in blue), as in (Figure 1.2).

In the case of Dark-QED it is possible to have vacuum polarization (Fig-

ure 1.3(a)), electron self-energy (Figure 1.3(b)) between others, but having always in mind that up to here it has only been considered dark fermions.

In the same way for Dark-QED this kind of processes can occur, which are visible but in the second order the interaction terms produce visible photons ($(-i)^2\eta\bar{\Psi}(x)\Psi(x)\gamma^\mu B_\mu(x)\bar{\Psi}(y)\Psi(y)\gamma^\nu A_\nu(y)$), as in Figure 1.4. This would be new phenomena, beyond the Standard Model and which could explain the excess of luminosity found in the center of the galaxy.

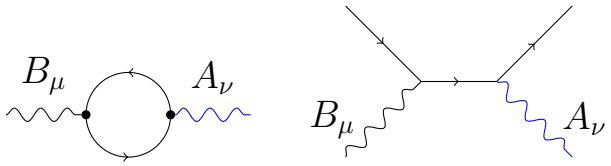

Figure 1.4: Interaction term $(-i)^2\eta\bar{\Psi}(x)\Psi(x)\gamma^\mu B_\mu(x)\bar{\Psi}(y)\Psi(y)\gamma^\nu A_\nu(y)$ diagrams. This kind of process could account for the phenomena observed in the center of the galaxy, the excess of luminosity which it is thought is a product of dark matter interactions leading to visible photons.

1.3 Vertex correction calculations

The leading contribution for the form factors in 1.14 would be $F_1 = 1$ and $F_2 = 0$ while loops will give contributions to F_1 and F_2 at order α and higher.

As can be seen in [59] the problem of calculating the quantum corrections of the electron magnetic moment can be reduced to compute the form factor, due to the relation between g and F_2

$$g = 2 + 2F_2(0). \tag{1.17}$$

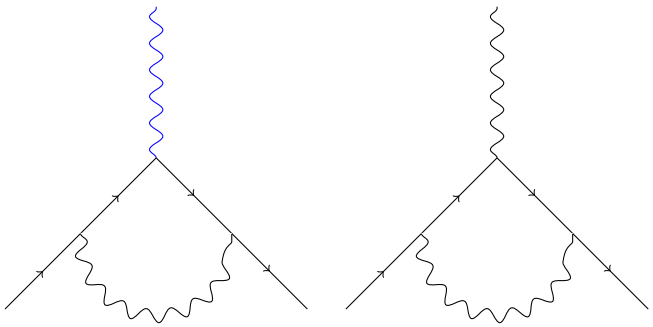

(a) Kinetic mixing term of order η

(b) Kinetic mixing term of order 1 (no mixing)

Figure 1.5: Vertex diagram for dark QED and kinetic mixing interactions

There are other terms that will also contribute to this calculation. As can be seen in Figure 1.2(a), for the interaction Lagrangian there is a term that only involves dark matter, that is a dark photon in the vertex coming from a dark matter annihilation which would not be perceptible for us but which contribution cannot be neglected. The matrix element and therefore the integral under the loop, is going to be the same for both diagrams in Figure 1.5, with the only difference given by the kinetic mixing value that brings the mixed diagram in Figure 1.5(a).

In this case the Feynman rules that contribute to the form factor related to the electron magnetic moment, considering the notation for graph 1.16 will be:

$$i\mathcal{M}'^{\mu} = (-\eta)\bar{u}(q')\int \frac{d^4l}{(2\pi)^4}\frac{g_{\alpha\beta}\gamma^{\alpha}\left(\not{k}+\not{l}+m_{\Psi}\right)\gamma^{\mu}\left(\not{l}+m_{\Psi}\right)\gamma^{\beta}}{\left[(l-q)^2-m_B^2+i\epsilon\right]\left[(l+k)^2-m_{\Psi}^2+i\epsilon\right]\left[l^2-m_{\Psi}^2+i\epsilon\right]}u(q). \tag{1.18}$$

This calculation has been performed extensively in [59] and for this same case in [15] so it can be checked that after some algebra, the corresponding contribution for the anomalous magnetic moment (going as $\sigma^{\mu\nu}p_\nu$) is:

$$F_2(k^2) = (\eta)8im_\Psi^2 \int_0^1 dx\, dy\, dz\delta(x+y+z-1) \int \frac{d^4l}{(2\pi)^4} \frac{z(1-z)}{(l^2-\Delta+i\epsilon)^3}, \quad (1.19)$$

plus other terms that do not contribute. For Δ we have

$$\Delta = -xyk^2 + (1-z)^2 m_\Psi^2 + m_B^2 z. \quad (1.20)$$

Following the description from [59] and [15], the form factor is obtained:

$$F_2(k^2) = \frac{\eta}{4\pi^2} \int_0^1 dx\, dy\, dz\delta(x+y+z-1) \frac{z(1-z)}{(1-z)^2 + \kappa^2 z - xy\frac{k^2}{m_\Psi^2}}, \quad (1.21)$$

where $\kappa = \frac{m_B^2}{m_\Psi^2}$. This result is the typical QED one, but for the present case there is a mass associated to the dark photon.

It is interesting to study some limits for this result; when $k_\mu \to 0$ the form factor takes the form:

$$F_2(0) = \frac{\eta}{4\pi^2} \int_0^1 dx\, dy\, dz\delta(x+y+z-1) \frac{z(1-z)}{(1-z)^2 + \kappa^2 z} \quad (1.22)$$

If were not by the term associated to the dark photon mass this result would be a finite integral, this is the case of a massless dark photon. If we

consider $e \neq 1$ and $\eta = 1$ as it is usual in QED we get the known result obtained by Schwinger, Feynman and Tomonaga:

$$F_2(0) = \frac{\alpha}{\pi} \int_0^1 dx\, dy\, dz \delta(x + y + z - 1) \frac{z}{(1 - z)} = \frac{\alpha}{2\pi}. \tag{1.23}$$

Remembering eq. (1.17) then

$$g = 2 + \frac{\alpha}{\pi} = 2.00232, \tag{1.24}$$

known as the electron anomalous magnetic moment. Going back to Dark QED the result would be:

$$F_2(0) = \frac{\eta}{4\pi^2} f(\kappa), \tag{1.25}$$

for the process in Figure 1.5(a) in where a visible photon is present in the vertex. For the case in which only dark matter is involved (Figure 1.5(b)) the proceeding is the same, getting the same integral. The only difference is given by the dependency in the kinetic mixing variable η, so it can be written in reference to Figure 1.5

$$F_2^a(0) = \frac{\eta}{4\pi^2} f(\kappa), \quad F_2^b(0) = \frac{1}{4\pi^2} f(\kappa). \tag{1.26}$$

The gyromagnetic factors for both diagrams are related due to this function, turning out to be

$$2F_2^a(0) = \frac{\eta}{2\pi^2} f(\kappa) = g_\Psi - 2, \tag{1.27}$$

$$2F_2^b(0) = \frac{1}{2\pi^2} f(\kappa) = g'_\Psi - 2, \tag{1.28}$$

thus

$$g_\Psi - 2 = \eta \left(g'_\Psi - 2 \right), \tag{1.29}$$

giving a relation between the correction in the dark sector to that for the interaction with the visible photon. Higher order contributions, as showed in Figure 1.6 are not considered. For the first case, Figure 1.6(a) the contribution would be of order η^2 (besides of having a different integral) and for the last case, Figure 1.6(b) of order η^3 growing with each mixed vertex.

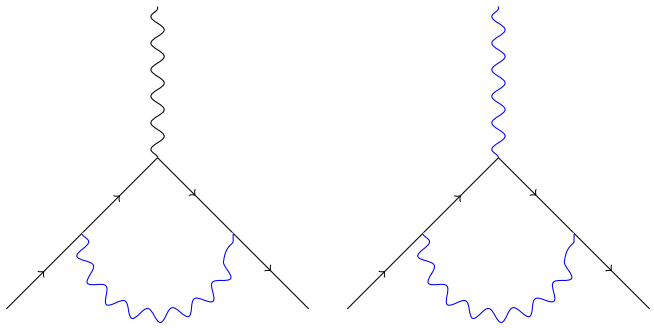

(a) Kinetic mixing term of order η^2

(b) Kinetic mixing term of order η^3

Figure 1.6: Vertex diagram for dark QED and kinetic mixing interactions at higher orders for the kinetic mixing parameter η.

We considered a very small kinetic mixing so only contributions up to order η were taken into account.

1.4 Results

The integral, function $f(\kappa)$ can be obtained using Mathematica giving, in terms of the ratio between the masses of the dark photon and dark fermion

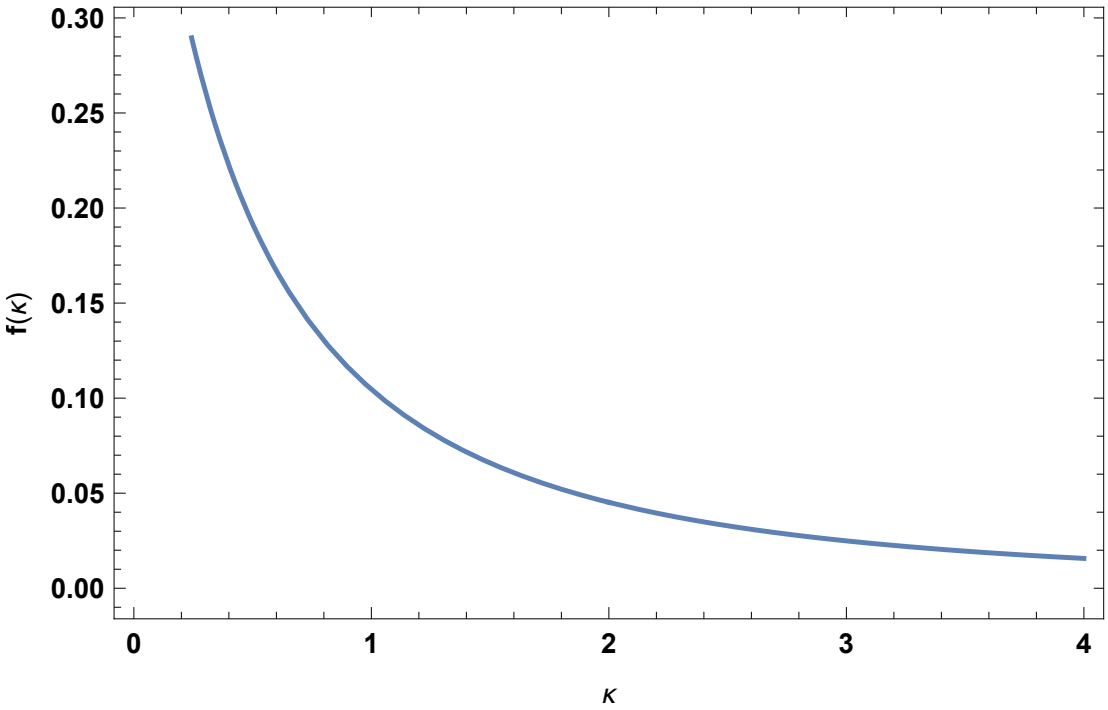

Figure 1.7: Behaviour of $f(\kappa)$ in terms of κ. Here we can see the behaviour after $\kappa = 1$ which means a photon with a mas higher than the mas of the fermion. This is completely different from what we know from QED so this behaviour shows utterly new physics.

$$f(\kappa) = -\frac{\kappa\left(2-4\kappa^2+\kappa^4\right)}{\sqrt{4-\kappa^2}}\tan^{-1}\left(\frac{\sqrt{4-\kappa^2}}{\kappa}\right)+\frac{1}{2}\left[1-2\kappa^2+2\kappa^2(\kappa^2-2)\ln\kappa\right] \tag{1.30}$$

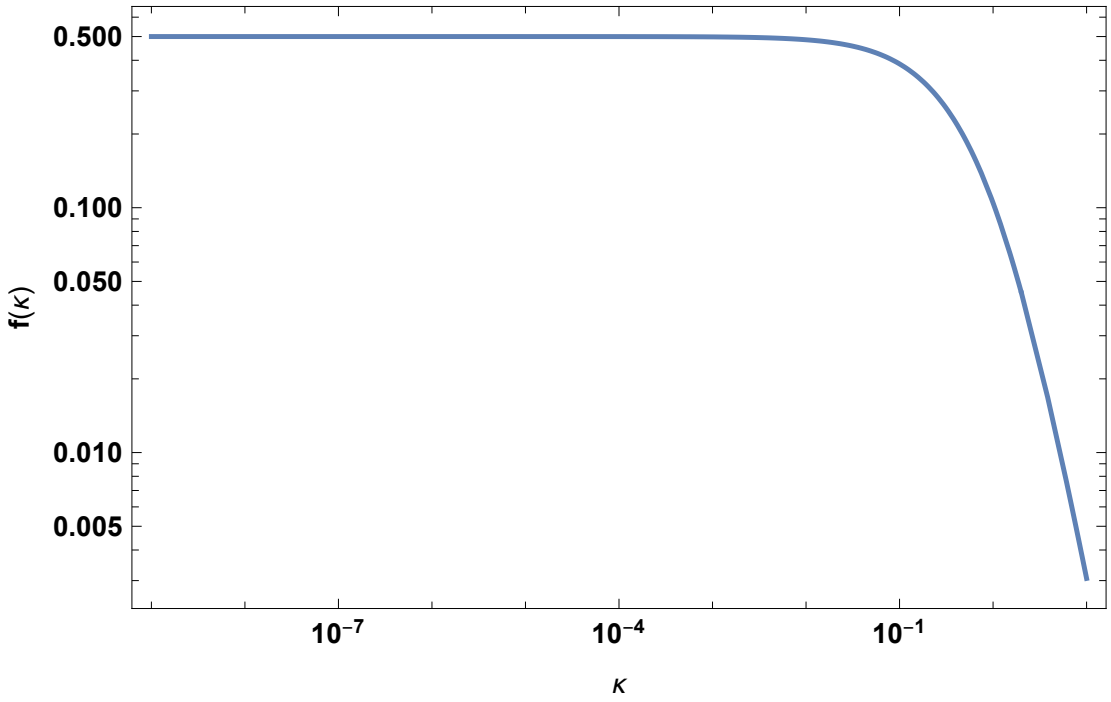

Figure 1.8: Behavoiur of $f(\kappa)$ in terms of κ as a log-log plot. In this case there is an abrupt decrease of the curve for $\kappa \sim 1$. This limit represents the behaviour of a dark photon with a mass similar in magnitude to the mass of a dark fermion, where the ratio κ is close to one. The inferior limit, for a dark photon mass going to zero or with a mas much smaller than the mass of the dark fermion, the function $f(\kappa)$ reaches the value $\sim 1/2$, which is the value known for visible QED.

As can be seen in Figure 1.7 this function is well defined near 2, which

is not obvious from eq. (1.30). In Figure 1.8 the value approximates to $\frac{1}{2}$ for small values of κ, being this the value expected for QED (and a massless dark, hidden photon).

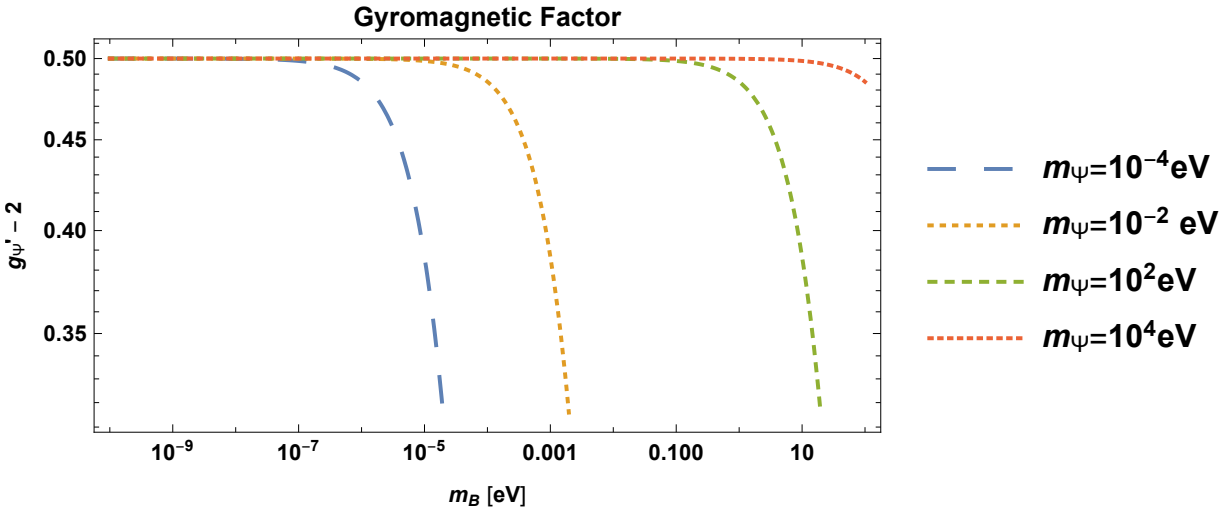

Figure 1.9: The different values of $f(\kappa) = g'_\Psi - 2$ in terms of hidden photon mass (m_B) for different values of the dark fermion mass m_Ψ, in log-log scale. It can be observed that all the functions go to $\frac{1}{2}$ for small hidden photon mass, as expected.

Thinking in the process shown in Figure 1.5(b), a dark vertex, we study the possible values for the gyromagnetic factor $g'_\Psi - 2$ in terms of the dark photon mass and for different values of the dark fermion. Seems pretty clear from Figure 1.9 that higher the dark fermion mass, it is easier for the dark photon to reach the QED expected value, even for hidden photon mass of order 1, in the case of fermion mass $\approx 10^4 eV$. There is actually a correspondence between the hidden photon mass and the dark fermion mass

for the gyromagnetic value to reach $\frac{1}{2}$, the photon mass must be of the same order or smaller than the fermion one, approaching the limit $\kappa \to 0$. In the cases of very small dark fermion mass the gyromagnetic factor drops fast around $\kappa \approx 1$.

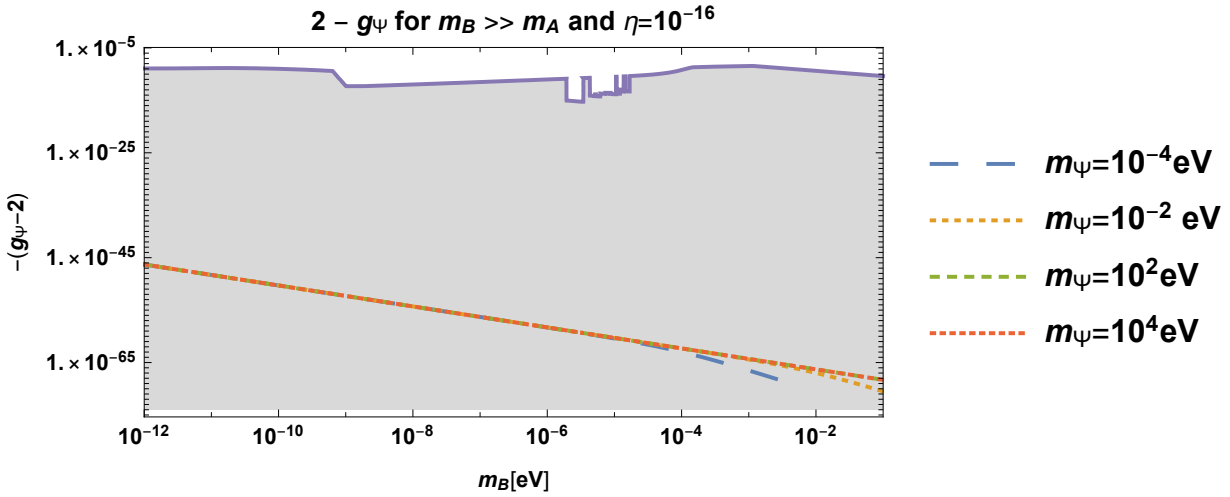

Figure 1.10: Log Log plot for the gyromagnetic factor $g_\Psi - 2$, this is the case the visible photon interacts with the dark fermion, in terms of the hidden photon mass and for $m_A \approx 10^{-27} eV$.

Now, let us consider the process which involves a visible external photon, Figure 1.5(a), it should be the most interesting one because it is this process that can be observed, in contraposition with the dark external photon case (Figure 1.5(b)).

In this case $g_\Psi - 2$ is negative (see [15]) due to the sign of η. Then, $2 - g_\Psi$ is studied, for $\eta = 10^{-16}$, for this value of η and smaller we are located inside the allowed parameter space (grey area in Figure 1.10) for parameters to be

detected as Dark Matter.

The behaviour is similar up to 10^{-4} eV for the hidden photon mass and over that the curves split around the mass of each fermion, $g_\Psi - 2$ is going to be small for each of them.

Chapter 2

Measuring the boiling point of vacuum of quantum electrodynamics

2.1 Introduction

It is not a new idea to establish that the laser has revolutionised many areas of science and society. These light sources create unique and sometimes extreme laboratory conditions transforming the way science is made and enabling trillions of dollars in commerce.

A new laser revolution is under way with pulsed petawatt-class lasers that deliver nearly 100 times the total world's power concentrated into a pulse that lasts less than one-trillionth of a second [51].

We will show and explain some of the phenomenology and calculations related to nonlinear processes in quantum electrodynamics, experiments which have made the efforts to measure the theory in the non-perturbative region.

2.2 Historical facts in High Intensity Laser experiments

It is known that Quantum Electrodynamics (QED) is a successful theory. It has been tested with outstanding precision in numerous experiments. This fact motivates to go further and test the theory under more challenging conditions as the one that can be found in intense background electromagnetic field. There are some observables that are not accesible by means of perturbation theory, the Breit Wheeler process –the creation of massive particles from massless photons– is one of these observables. It has not been observed due to the difficulty to prepare colliding beams of gamma rays, however there is a related nonlinear process which would be possible to observe using intense beams.

The first attempt of measuring strong field effects in QED was done at the SLAC E144 experiment in 1997 [22]. They demonstrated for the first time the process of turning light into matter or "sparkling the vacuum". At the Stanford Linear Accelerator Center (SLAC), the 20-physicist collaboration focused an extremely intense laser beam at a beam of high-energy electrons, to create a field as close as possible to critical, where the fields are so strong

that their energy can be converted directly into the creation of e^+e^- pairs. . The collaboration started with a short-pulse glass laser that packs a half-trillion watts of power into a beam measuring just 6 micrometers across at its narrowest point, resulting in extraordinary intensities (0.5×10^{18} W/cm^2), the aim was to study QED near the critical electromagnetic field [5].To increase the energy of the photons, the team collided the pulses with SLAC's 30-micrometer-wide pulsed beam of high-energy electrons. When the laser photons collided head-on with the electrons, they got a huge energy boost, changing them from visible light to very high-energy gamma rays. These high-energy photons then rebounded into the path of incoming laser photons, interacting with them, a collision with four laser photons concentrated enough energy in one place to produce electron-positron pairs. Such particle pairs are often spawned in accelerator experiments that collide other particles at high energies, and photons produced in the collision are the immediate source of the pairs. But in those experiments, at least one of the photons involved is "virtual"–produced only for a brief moment in the strong electric field near a charged particle of matter. The SLAC experiment marks the first time matter has been created entirely from ordinary photons.

Nevertheless in this case they were not able to reach non-perturbative regime. Nonlinear Compton Scattering [13], light by light scattering, pair production, and trident process were measured, but all of them out the strong field regime.

There are two ways to measure how strong is a field. One of them is only possible by going above the critical field, this is the case in where the

difference in the potencial associated to the electric field is bigger in one Compton wavelength than the rest energy of the electron.

The second case occurs when the potencial difference is bigger in one wavelength than the rest energy of the electron. This is also called the "static limit", and it is defined by the laser nonlinearity parameter:

$$\xi = \frac{eE}{m_e w} = \frac{m_e}{w}\frac{E}{E_c}, \tag{2.1}$$

where m_e is the mass of the electron, w is the laser frequency, e is the electron charge, E is the electric field and E_c is the Schwinger critical field. This parameter represents the work, referred to $m_e c^2$, performed by the field over the wavelength. When ξ is small the processes have the smaller amount possible of photons, the probabilities related are perturbative and the plane wave plays the role of individual photons. When the parameter ξ is of order or bigger than 1 the processes become multiphoton and the probabilities have a nonlinear dependence on the field or on the photon-number density.

Recently there is new interest in study QED at extreme conditions. The facilities are in construction and new extreme intensities are planned to reach in the near future. This would allow to get closer to the critical field and intensity of QED theory and observe interesting processes in the non-perturbative regime. It is expected that new lasers would reach the 100PW power and intensities near 10^{25} W/cm^2 at the focussing point.

Another related experiment is going to take place at DESY (Deutsches Elektronen-Synchrotron) where an electron beam of 17.5GeV and a laser of

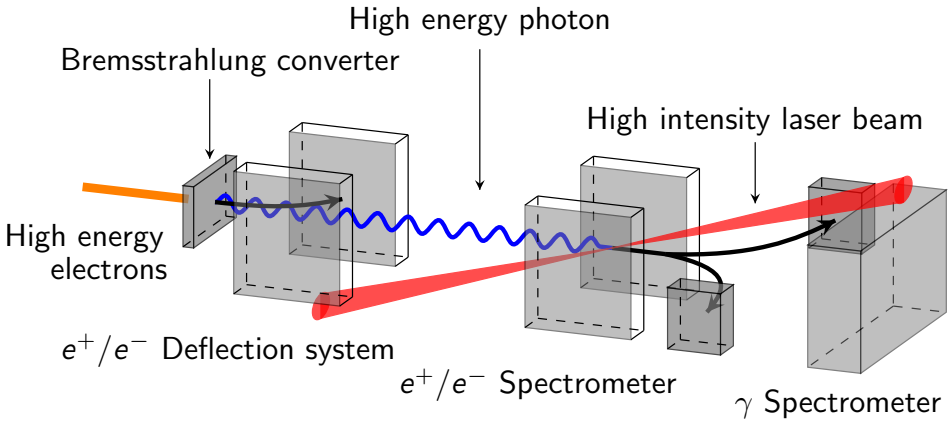

Figure 2.1: Sketch of an experiment to produce high energy photons by bremsstrahlung conversion in a high-Z thin target and to cross them with a laser beam to let them decay into electron-positron pairs. Switching off the laser allows for a determination of the bremsstrahlung spectrum. Removing the target allows in addition for the study of High Intensity Compton Scattering (HICS) , followed by OPPP, and of the one-step trident process.

expected $10^{20}\mathrm{W/cm}^2$ peak at the focussing point are going to be brought into collision. It is expected to see pair production around $3 \times 10^{18} \frac{\mathrm{W}}{\mathrm{cm}^2}$ in the non-pertubative regime [34]. This second chapter and the project related [34] is the result of the work under the supervision of Professor Andreas Ringwald and in collaboration with Anthony Hartin, in the physics case of this experiment. We worked on the rates of electron positron pair production for the Luxe experiment (Laser und XFEL.eu experiment) and we propose a completely new experimental set up in order to produce high energy photons

by Bremsstrahlung (see Figure 2.1). The results here presented for electron positron pair production are under the consideration of this experimental set up and the parameters related to it.

The theory behind SLAC experiment and in the most recent predictions for pair production rates [34] is the one orchestrated in the 60's by Narozhny, Nikishov and Ritus [58]. In this theory it was considered a circularly polarised laser beam in order to simplify the calculations. Nowadays, new methods are used to obtain the rates of electron positron pair production, the focussing of the laser, the pulse length and geometry considerations are taken into account to have in mind non-ideal effects [19, 18, 17, 16, 49]. This effects would considerably affect the rates and even suppressed them at certain level. In this sense there is much to be done yet.

2.3 QED processes in the background of a high intensity electromagnetic wave

For nonlinear Compton Scattering the scenario thought is a High Intensity laser beam brought into collision with an electron beam. It is expected that at High intensities and due to the effective mass of the electrons in the background of the laser beam, the Compton edge will suffer a substantial red-shift [35] in the photon spectrum (see Figure 2.4). Emission rates in this case reach their global maxima at this edge, followed by smaller peaks corresponding to higher harmonics. At the SLAC E-144 experiment the

method chosen to create high energy photons was this one, and the Compton edge play a crucial role at the time to get the higher energy possible for the hard (high energy) photon. Pair production was observed also at SLAC experiment but it was related to a trident process in which both, high energy electrons and photons can interact with the laser photons. In this process a pair $e^{-}e^{+}$ is produced. In their case and as there was no existent theory related to the process [5], the rates were estimated as a two step process. The first step involves high energy virtual photon by nonlinear Compton Scattering, then this photon will interact again with the laser photons as a nonlinear Breit-Wheeler pair production. Due to the Compton edge the higher intensities for the higher photon are suppressed and therefore also the pair production rate.

Some definitions

The abundance of strong field QED processes can be categorised in two groups: loop and tree-level processes. Heisenberg-Euler effective Lagrangian is obtained by summing in all orders the loop diagram (as vacuum polarization) at low energy, which later can be used to obtain the non-perturbative mechanism of spontaneous pair production in vacuum [35]. It can be found in the literature [35, 5, 58, 50] a diverse way to define the invariants and the rates for non-linear Compton Scattering, also named as the emission of a photon by an electron in an intense electromagnetic field. In this case we will follow the notation of [50], only varying some definitions for the

parameters in a convenient way and only showing here the most essential expressions as the rates and the definition of the parameters involved in the process itself. The derivation of this formulae can be found extensively in [58].

In papers previous to [50] ([52, 53]) different processes probabilities in QED were calculated for a linearly polarized plane wave. The case for circularly polarized wave as it is showed here allows much simpler expressions in terms of Bessel functions and one integral is dropped in comparison with the linearly polarized case. Finally, this formulation makes possible to understand and analyse physical questions as the dependency of the processes rates in the frequency of the wave or in the number of photons absorbed in the process.

The solution of the Dirac equation in the field of the circularly polarized wave has the form (see [52, 53, 50]):

$$\psi_p = \left[1 + e\frac{\hat{k}\hat{A}}{2(kp)}\right] u(p) \exp\left[ie\frac{(a_1 p)}{(kp)}\sin\varphi - ie\frac{(a_2 p)}{(kp)}\cos\varphi + i(qx)\right], \quad (2.2)$$

where p_μ is a constant four-vector determining the state, $p^2 = -m^2$, $q_\mu = p_\mu - \frac{e^2a^2}{2(kp)}k_\mu$ is the average kinetic momentum of the particle ("quasimomentum"), $q^2 = -m_*^2 = -m^2(1 + \frac{e^2a^2}{m^2})$, m_*^2 is the "effective" mass of the particle in the field. This effect is also referred to as the "dressing" of the electron in the background of the laser.

The probabilities showed below contain the differential probabilities and

the probabilities in terms of the number of photons absorbed during the specific process.

Photon emission

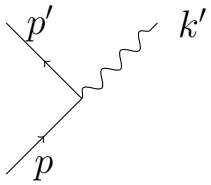

Figure 2.2: Photon emission from an electron, the relation for the momentum is $p^2 = -m^2$, $q_\mu = p_\mu - \frac{e^2a^2}{2(kp)}k_\mu$ and this represents the process $nk+q = q'+k'$, the absorption of "n" laser photons, resulting a high energy photon k'.

The probability of emission of a photon by an electron per unit volume per unit time, as a result of computing the matrix element for the transition of an electron from the state ϕ_p into the state $\phi_{p'}$ emitting a photon k' (see Figure 2.2), turns out to be equal to

$$\begin{aligned} F_{Compton}(\chi_e,\xi) &= \frac{e^2m^2n_\gamma}{16\pi q_0}\sum_{n=1}^{\infty}\int_0^{u_n}\frac{du}{(1+u)^2}\times \\ &\qquad \left\{-4J_n^2(z)+\xi^2\left(2+\frac{u^2}{1+u}\right)(J_{n-1}^2+J_{n+1}^2-2J_n^2)\right\} \\ &= \frac{e^2m^2n_\gamma}{16\pi q_0}\int_0^{u_n} du f_{Compton}(\chi_e,\xi,u)_n \end{aligned} \tag{2.3}$$

it depends on the n number fo photons absorbed from the field. The emission of a photon of momenta k' is only possible if more than one photon with momenta k is absorbed. This process can happen due to the quasimomenta definition for the electron un the background of the laser.

The dependency on the Bessel functions is a manifestation of the nonlinearity of the process. Another invariant is the variable u and the upper limit in the integral u_n together with the Bessel function argument z are defined as follow:

$$u = \frac{(kk')}{(kq')}, \quad u_n = \frac{-2n\,(kq)}{m_*^2} = 2\frac{(n\,\chi_e)}{\xi(1+\xi^2)}, \quad z = \left(\frac{\xi^2\sqrt{1+\xi^2}}{\chi_e}\right)\sqrt{u(u_n-u)}. \tag{2.4}$$

This probability, as well as the probability for a linearly polarized wave, depends on two invariants which have been chosen in the form

$$\xi = \frac{ea}{m}, \quad \chi_e = -\frac{\xi(kp)}{m^2} = e\frac{\sqrt{(F_{\mu\nu}p_\nu)}^2}{m^3}, \tag{2.5}$$

where a is the amplitude of the vector potential associated with the electromagnetic field and $F_{\mu\nu}$ is the amplitude of the intensity of the field.

The amplitude a is related to the average photon number density n_γ or with the average density η by the relation

$$a = \sqrt{\frac{n_\gamma}{\Omega}} = \frac{\sqrt{\eta}}{\Omega} \tag{2.6}$$

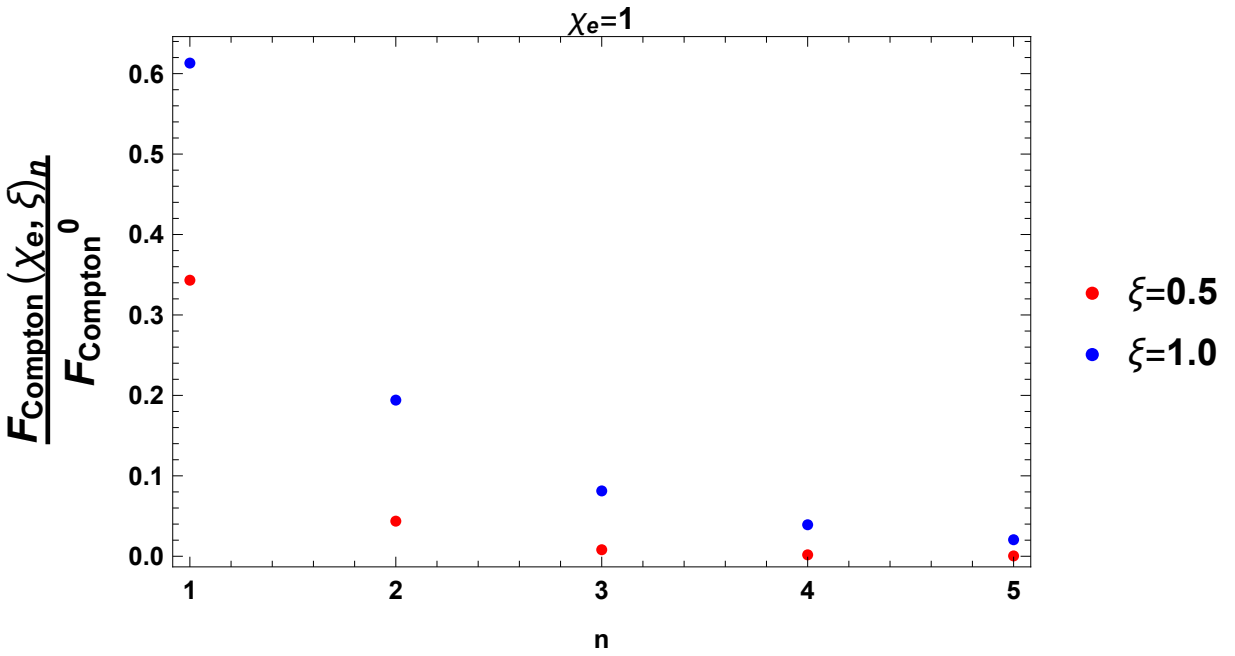

Figure 2.3: Probability emission distribution for $F_{Compton}(\chi_e, \xi)_n$, $F^0_{Compton} = \frac{e^2 m^2 n_\gamma}{16\pi q_0}$ in terms of n photons absorbed for a constant recoil parameter $\chi_e = 1$ and laser parameter $\xi = 0.5$ (red) and $\xi = 1.0$ (blue). We can easily understand from this, that the rates are smaller of each new photons absorbed and this will mean later that the most important contributions will come from the first harmonic.

The electron recoil parameter χ_e is written in a more suitable way to make the calculations, in terms of the electron beam energy $p \to E_e$ and the laser photon energy $k \to w$.

$$\chi_e = \frac{E_e}{m}\frac{w}{m}(1 + \cos\theta)\xi \tag{2.7}$$

The parameter χ_e constitutes the work performed by the field over the

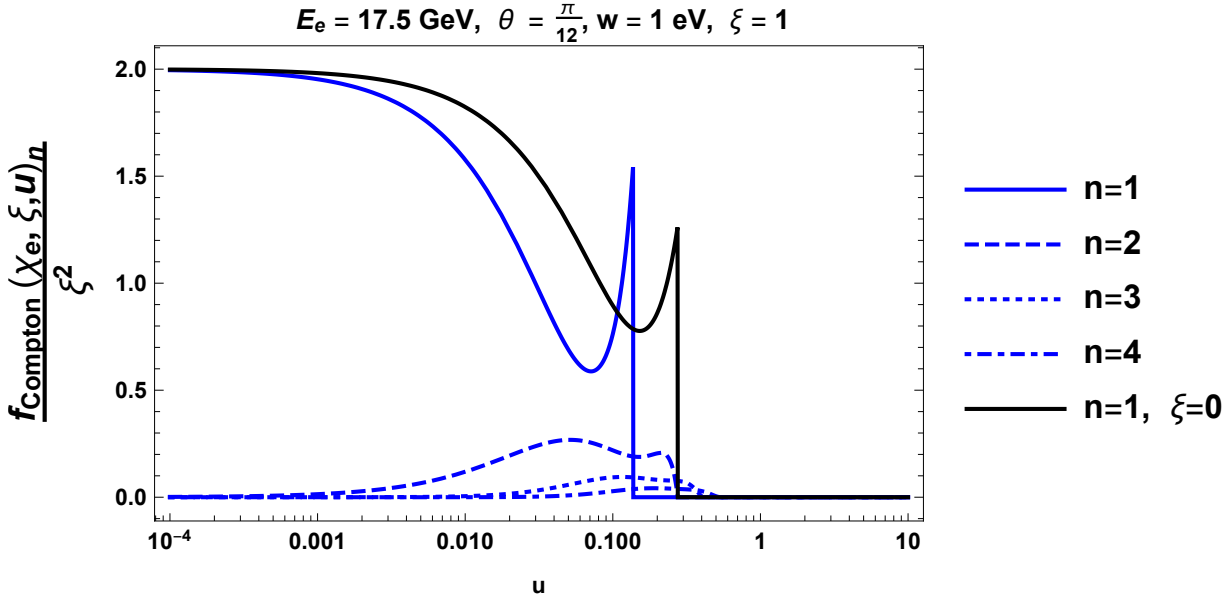

Figure 2.4: Probability emission distribution for $f_{Compton}(\chi_e, \xi, u)_n/\xi^2$ in terms of the variable u for different values of n photons absorbed for a constant recoil parameter $\chi_e = 1$ and laser parameter $\xi = 0$ (black) and $\xi = 1.0$ (blue).

Compton length in the particle rest system, it is responsible on the magnitude of the nonlinear effects, which are optimal for the regime ξ much bigger than 1 at $\chi_e \sim 1$.

As can be seen in Figure 2.3 the rate of nonlinear Compton Scattering decreased with the higher harmonics. This will cause that the peak contribution will come from the first harmonic, which has the smaller high energy photon emission energy and this will make the pair production rate to be smaller in the case of the trident process as expected in SLAC experiment. This is one of the main reasons why in the case of LUXE experiment an-

other way to produce the high energy photon was proposed, Figure 2.1. It is easier to see from Figure 2.4 were the shift in the Compton edge is visible. The mass shift caused by the laser parameter increasing has as a result the shift in the energy of the Compton edge. To study the different rate for a fixed value of recoil parameter allow us to study in a qualitatively way the probability of the process.

Pair creation

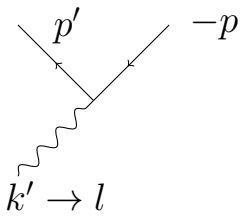

Figure 2.5: Pair production by a photon in the background of an intense electromagnetic wave, the relation for the momentum is $p^2 = -m^2$, $q_\mu = p_\mu - \frac{e^2a^2}{2(kp)}k_\mu$ and this represents the process $nk + k' = q + q'$.

If in (eq. (2.3)) the replacement $p \to -p$, $k' \to -l$ is carried out, and reverse the common sign of the expression we can obtain the probability for the production of a pair by a photon of momentum l evaluated per unit volume and per unit time:

$$F_{pp}(\chi_\gamma,\xi) = \frac{e^2m^2n_\gamma}{16\pi l_0}\sum_{n>n_0}\int_1^{v_n}\frac{dv}{v\sqrt{v(v-1)}}\times$$
$$\left\{2J_n^2(z)+\xi^2\left(2v-1\right)\left(J_{n-1}^2(z)+J_{n+1}^2(z)-2J_n^2(z)\right)\right\}$$
$$= \frac{e^2m^2n_\gamma}{16\pi l_0}\int_1^{v_n} dv f_{pp}(\chi_\gamma,\xi,v)_n \tag{2.8}$$

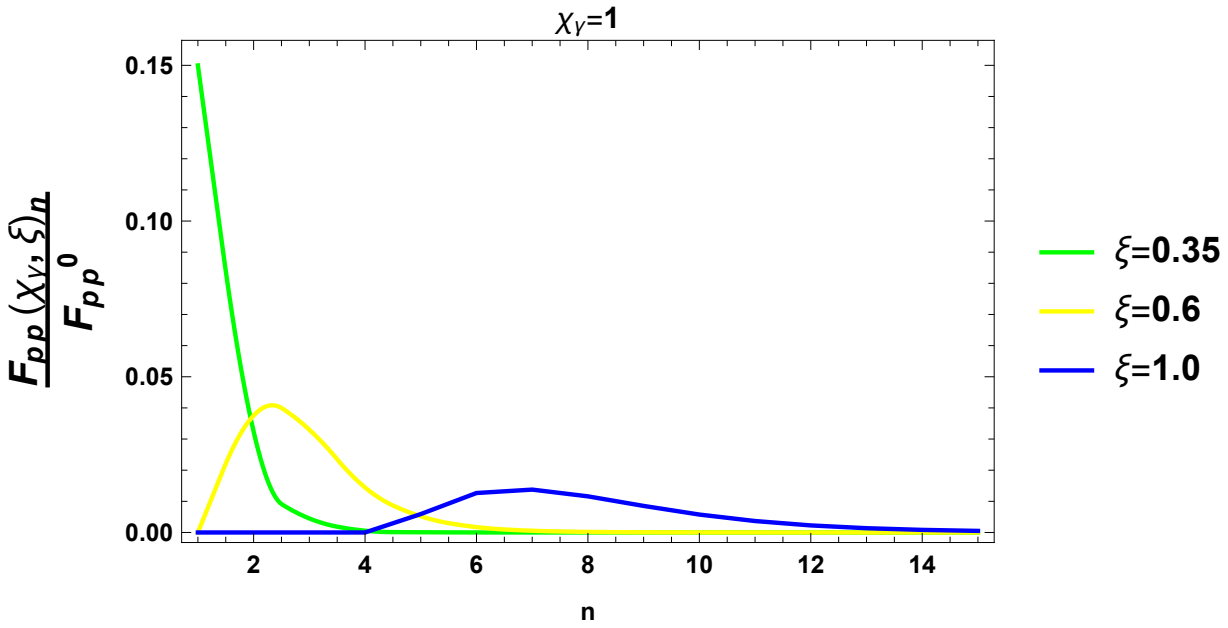

Figure 2.6: Probability emission distribution for $F_{pp}(\chi_\gamma,\xi)_n$, $F_{pp}^0 = \frac{e^2m^2n_\gamma}{16\pi l_0}$ in terms of n photons absorbed for a constant recoil parameter $\chi_\gamma = 1$ and laser parameter $\xi = 0.35$ (green), $\xi = 0.6$ (yellow), and $\xi = 1.0$ (blue).

$$v = \frac{(kl)^2}{4(kq)(kq')}, \quad v_n = \frac{n}{n_0}, \quad n_0 = -\frac{2m_*^2}{(kl)} = \frac{2\xi(1+\xi^2)}{\chi_\gamma}, \tag{2.9}$$

$$z = 4\left(\frac{\xi^2\sqrt{1+\xi^2}}{\chi_\gamma}\right)\sqrt{v(v_n - v)}. \tag{2.10}$$

This probability, as well as the probability for a linearly polarized wave, depends on two invariants (being the first the laser parameter ξ) which have been chosen in the form

$$\chi_\gamma = \xi\frac{(kl)}{m^2} = e\frac{\sqrt{(F_{\mu\nu}\, l_\nu)^2}}{m^3}. \tag{2.11}$$

And also, for convenience can be written in terms of the kinematic parameters in the process

$$\chi_\gamma = \frac{\omega}{m}\frac{w}{m}(1+\cos\theta)\xi \tag{2.12}$$

being ω the high energy photon energy in eV and θ the collision angle.

When the nonlinearities are present, for a n number of photons, the cross section gets lowered (see Figure 2.7 and also Figure 2.6). This is an immediate effect of the mass shift effect. As can be seen in eq. (2.9) for higher laser parameters more and more photons are needed to create one pair. As a compensation for the effects due to the mass shift, the growing contribution of multi-photon terms [32], this allow the process to be possible even below the Breit-Wheeler threshold.

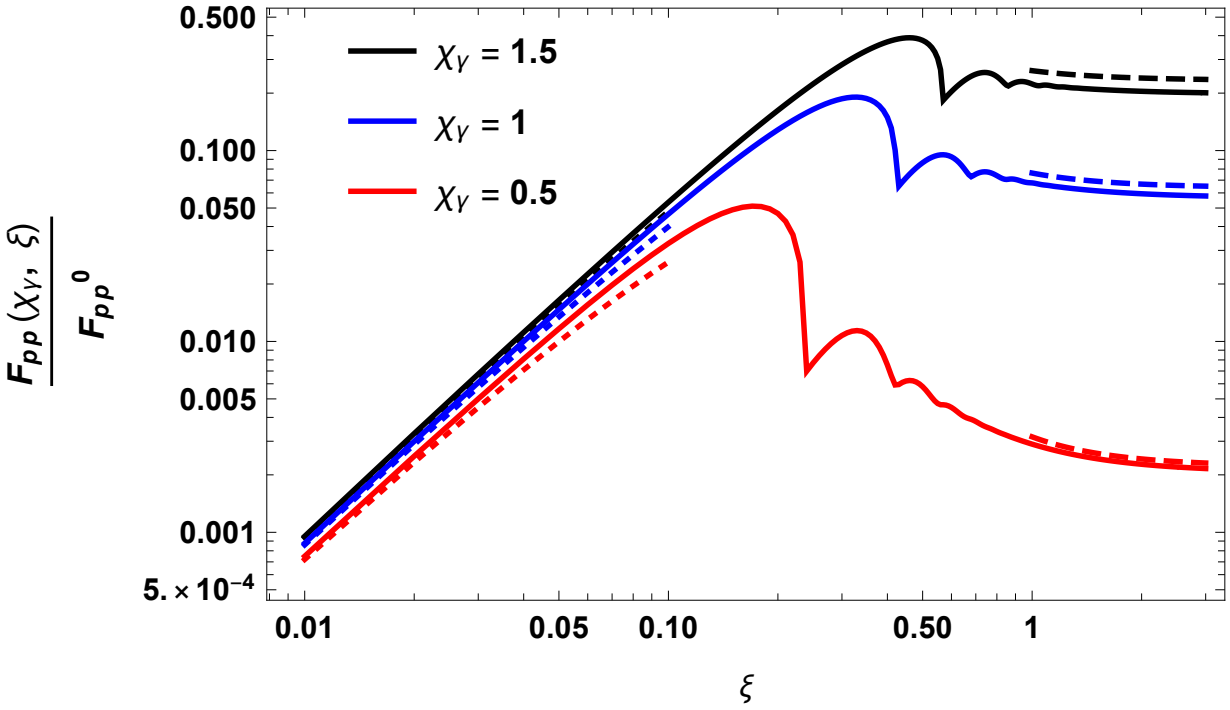

Figure 2.7: Probability $F_{pp}(\chi_\gamma, \xi)$ of pair production, $F^0_{pp} = \frac{e^2 m^2 n_\gamma}{16\pi l_0}$ in terms of n the laser parameter for a constant recoil parameter $\chi_\gamma = 0.5$ (red), $\chi_\gamma = 1$ (blue) and $\chi_\gamma = 1.5$ (black). The dashed line correspond in any case to the asymptotic value for the probability in 2.13.

The static limit

In the laser parameter, eq. (2.1) there is an interesting limit, in which the non-perturbative and nonlinear behaviour is observed. This parameter is bigger than one when the field of the process higher in magnitude than the critical Schwinger field. Also when the frequency is very small in comparison with the other parameters in ξ. In this case the number of photons involved in the process also increases to produce a pair and therefore the Bessel

function argument too, and for that the Bessel functions can be replaced by Debye's asymptotic expansion, for high order and argument. Then the integral and the summation are simplified to the next analytic formula

$$F_{pp}(\chi_\gamma,\xi)_{asymp} = F^0_{pp}\,\frac{3}{4}\sqrt{\frac{3}{2}}\chi_\gamma \exp\left[-\frac{8}{3\chi_\gamma}\left(1-\frac{1}{15\xi^2}\right)\right] \tag{2.13}$$

Expression (2.13) is only valid for $\xi \gtrsim \frac{1}{\sqrt{\chi_\gamma}} \gg 1$, and $F^0_{pp} = \frac{e^2m^2n_\gamma}{16\pi l_0}$. This expression represents the dashed lines in Figure 2.7 . For laser parameter much smaller than 1 ($\xi \ll 1$), the behaviour is as expected, the rate depends quadratically on the coupling constant, thus ξ (see Figure 2.7, dotted lines) as can be expected from perturbation theory.

Bremsstrahlung spectrum

The case of the Bremsstrahlung spectrum can be approximated as

$$\omega\frac{dN_\gamma}{d\omega} \sim \frac{X}{X_0}\left(\frac{4}{3}-\frac{4}{3}\frac{\omega}{E}+\left(\frac{\omega}{E}\right)^2\right) \tag{2.14}$$

Instead of obtaining the high energy photons by means of nonlinear Compton scattering, we propose a laser assisted one photon Bremsstrahlung pair production (OPPP) (see Figure 2.1), and in order to obtain the rate of pairs produced we integrate the rate of pair production in this spectrum.

According to [9] the integral over the bremsstrahlung spectrum can be obtained from the next expression

$$\int_0^{E_e} F_{pp}(\chi_\gamma(\omega),\xi)\,\frac{dN_\gamma}{d\omega}\,d\omega \tag{2.15}$$

Integral for the complete rate

In the case of the complete rate the procedure followed is;

$$\begin{aligned} N_{OPPP} =& \frac{e^+e^-pairs}{(electronbunch)*(lasershot)} \\ =& \int_0^{E_e}\left(\frac{1}{\omega}\right)\left[\frac{X}{X_0}\left(\frac{4}{3}-\frac{4}{3}\frac{\omega}{E}+\left(\frac{\omega}{E}\right)^2\right)\right]F_{pp}(\chi_\gamma(\omega),\xi)\,d\omega \\ =& \int_0^{E_e}\left(\frac{1}{\omega}\right)\left[\frac{X}{X_0}\left(\frac{4}{3}-\frac{4}{3}\frac{\omega}{E}+\left(\frac{\omega}{E}\right)^2\right)\right]\sum_{n>n_0}\int_1^{v_n}\frac{dv}{v\sqrt{v(v-1)}}F^0_{pp}\times \\ & \left\{2J_n^2(z)+\xi^2\,(2v-1)\left(J_{n-1}^2(z)+J_{n+1}^2(z)-2J_n^2(z)\right)\right\}d\omega, \end{aligned} \tag{2.16}$$

the integral, taken over ω can be seen in Figure 2.8 as the solid line, representing this entire calculation without approximations..

Integration for the limiting case $\xi >> 1$

Having in mind the result for $\xi >> 1$ from [58], the behaviour of the OPPP rate would be in such a way the the most important contribution comes from the neighbourhood of $\chi_\gamma = 1$, (see Figure 2.10), so the behaviour of the Bremsstrahlung spectrum is crucial around this limit, also the OPPP is suppressed in the limit $\xi >> 1$.

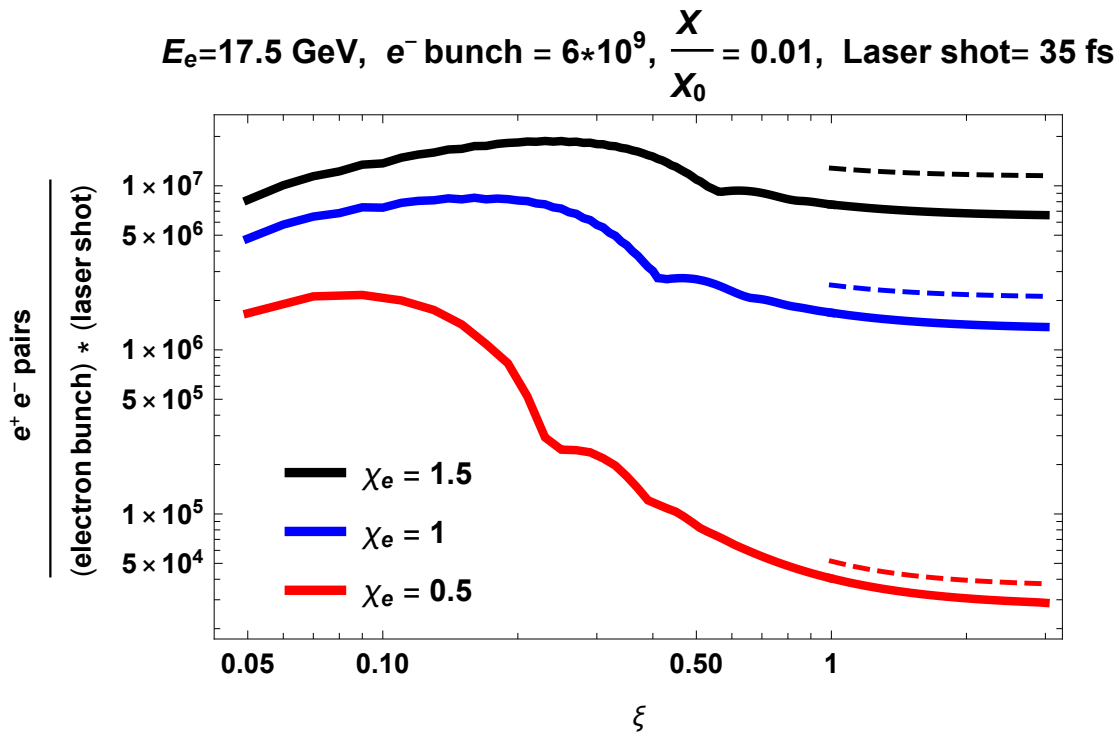

Figure 2.8: Number of e^+e^- pairs produced per electron bunch (6×10^9 electrons of energy $E_e = 17.5\,\mathrm{GeV}$) impinging on the converter target (thickness $X/X_0 = 0.01$) and per laser shot (duration 35 fs) crossed with the bremsstrahlung photons, as a function of the laser intensity parameter ξ, for different values of χ_e, from Equation (2.16). The dashed line shows the analytic prediction resulting from Equation (2.17), valid at $\xi \gtrsim 1/\sqrt{\chi_e} \gg 1$.

$$\frac{e^+e^-pairs}{(electronbunch) * (lasershot)} \tag{2.17}$$

$$= \int_0^{E_e} \left(\frac{1}{\omega}\right) \left[\frac{X}{X_0}\left(\frac{4}{3} - \frac{4}{3}\frac{\omega}{E} + \left(\frac{\omega}{E}\right)^2\right)\right] F_{pp}(\chi_\gamma(\omega), \xi)_{asymp}\, d\omega$$

$$= \int_0^{E_e} \left(\frac{1}{\omega}\right) \left[\frac{X}{X_0}\left(\frac{4}{3} - \frac{4}{3}\frac{\omega}{E} + \left(\frac{\omega}{E}\right)^2\right)\right] F^0_{pp}\, \frac{3}{4}\sqrt{\frac{3}{2}}\, \chi_\gamma \exp\left[-\frac{8}{3\chi_\gamma}\left(1 - \frac{1}{15\xi^2}\right)\right] d\omega$$

$$= \frac{X}{X_0}\frac{\alpha m^2 n_\gamma}{E}\frac{9}{128}\sqrt{\frac{3}{2}}\, \chi_\gamma^2 \exp\left[-\frac{8}{3\chi_\gamma}\left(1 - \frac{1}{15\xi^2}\right)\right]. \tag{51}$$

Here we have taken the asymptotic expression in eq. (2.13) and integrated it over the Bremsstrahlung spectrum, obtaining an analytic expression for the rate, which represents the dashed lines in Figure 2.10.

The rate of e^+e^- pairs

In order to get the number of pairs produced corresponding to every bunch of electrons, we take (eq. (2.15)) which can be written in terms of ω or χ_γ

$$\int_0^{\chi_e} w(\xi,\chi_\gamma)\frac{dN}{d\chi_\gamma}d\chi_\gamma \;=\; \frac{e^2m^2n_\gamma}{16\pi E_0}\int_0^{\chi_e}\frac{\chi_e}{\chi_\gamma}F(\xi,\chi_\gamma)\frac{dN}{d\chi_\gamma}d\chi_\gamma \tag{2.18}$$

and calculate the value of the prefactor

$$\frac{e^2\,m^2\,n_\gamma}{16\,\pi\,E_0}=\frac{\alpha\,m^2\,n_\gamma}{4\,E_0}. \tag{2.19}$$

We can write the invariants in term of the intensity:

$$\xi = 7.495\left(\frac{I}{10^{20}\,\frac{\mathrm{W}}{\mathrm{cm}^2}}\right)^{1/2}\left(\frac{1\,\mathrm{eV}}{\omega}\right) \tag{2.20}$$

$$\chi_e = 0.4985\,(1+\cos\theta)\left(\frac{E_e}{17.5\,\mathrm{GeV}}\right)\left(\frac{I}{10^{20}\,\frac{\mathrm{W}}{\mathrm{cm}^2}}\right)^{1/2}, \tag{2.21}$$

and get number for the rate of electron positron pair production in terms of a parameter of interest for the experiment laser, some values of it to have a reference are shown in Table 2.1.

It is important to remark that the result obtained in this chapter regard processes in the field of a plane **circularly** polarized electromagnetic wave. The probabilities for processes in the field of a linearly polarized wave can be checked in [58]. For that case the results are much more complex and the simplification carried in this case, thank to Debye's Asymptotic expansion cannot be done, only in limiting cases the expressions can be simpler.

For circularly polarized waves the probabilities are exact and straightforward, expressed in terms of Bessel functions which makes it much easier to study its rates and a number of physical quantities.

Intensity $[\frac{\mathbf{W}}{\mathbf{cm}^2}]$	χ_e (χ_γ)	ξ
$5\text{x}10^{18}$	0.219138	1.08125
$1\text{x}10^{19}$	0.309908	1.52911
$5\text{x}10^{19}$	0.692975	3.4192
$1\text{x}10^{20}$	0.980014	4.83548

Table 2.1: The laser intensity parameter ξ and the electron recoil parameter χ_e, as a function of the intensity, eq. (2.20) and eq. (2.21).

The probability of pair production for constant photon recoil parameter χ_γ depends essentially non monotonically on ξ, it can be seen the different maxima, becoming less pronounced for higher laser parameter ξ. This be-

haviour is intimately connected with the fact that pair production process possesses a threshold number of photons (eq. (2.9)) needed to be absorbed from the laser to create one pair, and which value increases with the growth of ξ. If the laser parameter increases (or the intensity), the minimum number of photons needed for the process to occur also will increase.

For higher ξ a larger number of terms drops out from the integral for $n = 1$ and up to $n \leq n_0$. The main contribution for small ξ come from $n = 1$, thus this term dropping out is easily noticeable in Figure 2.7 and Figure 2.8.

2.4 Results

In Figure 2.9 in can be appreciated that at least one pair would be measurable around $3 \times 10^{18} \frac{\mathrm{W}}{\mathrm{cm}^2}$. Here red dashed lines represent the asymptotic result after integration eq. (2.17) using eq. (2.20) and eq. (2.21) to express this result in terms of the intensity of the laser, which is much easier way to understand the results obtained from an experiment. Black dots represent the complete rate integrated under the Bremsstrahlung spectrum as shows eq. (2.16). The rate, for a fixed electron beam energy of $17.5GeV$ in terms of the intensity shows that for a peak intensity of $10^{20}W/cm^2$ the number of pair production is going to be around 10^6 pairs per bunch. In order to have an "error bar " we have considered the possibility of a deviation from the nominal value of the critical electric field of QED, being this of a 10% higher (green dashed lines) and lower (blue dashed lines). In both cases this shows

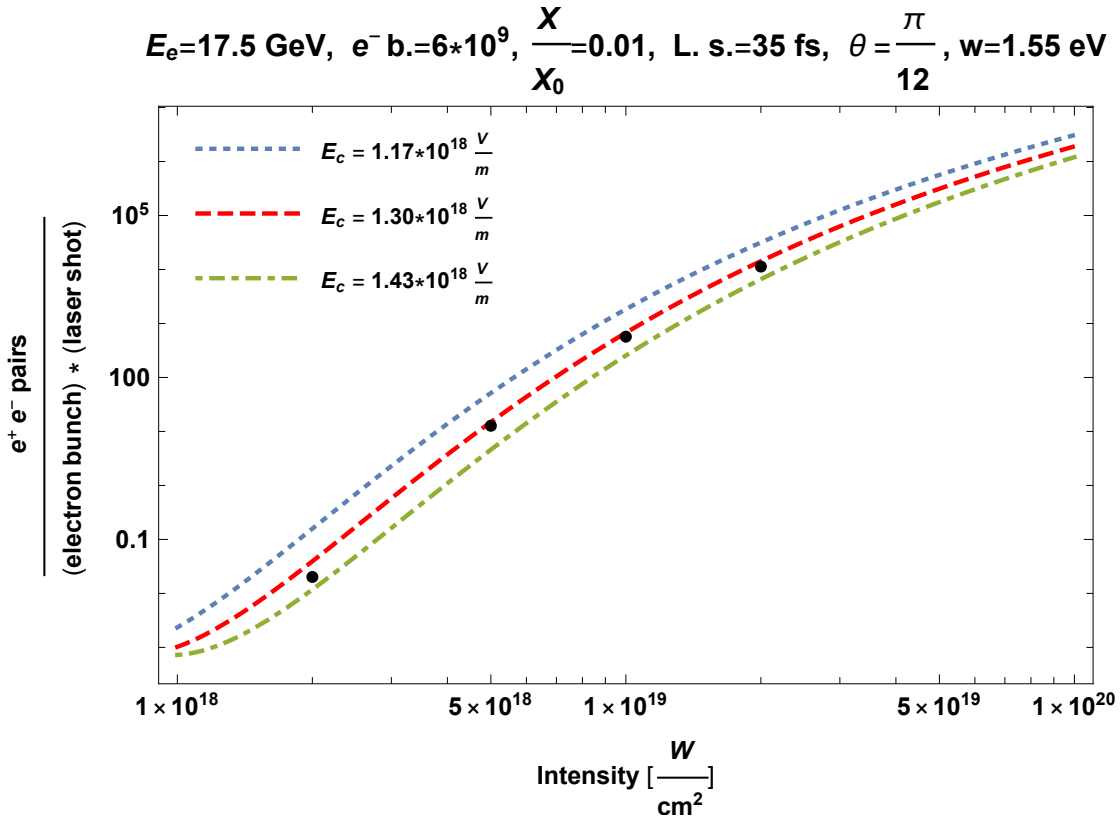

Figure 2.9: Number of e^+e^- pairs produced per electron bunch (6×10^9 electrons of energy $E_e = 17.5\,\mathrm{GeV}$) impinging on the bremsstrahlung target (thickness $X/X_0 = 0.01$) and per laser shot (duration 35 fs, laser frequency $\omega = 1.55\,\mathrm{eV}$) crossed with the bremsstrahlung photons at an angle of $\theta = \pi/12$, as a function of the laser intensity. The dashed line shows the analytic prediction resulting from 2.17, exploiting the relations 2.20 and 2.21. The dotted (dot-dashed) line shows the same analytic prediction, but for the case where the value of the Schwinger critical field E_c deviates by a 10 percent down (up) its nominal value.

a difference of around one order of magnitude for small intensities and this difference becomes smaller at intensities near $10^{20} W/cm^2$.

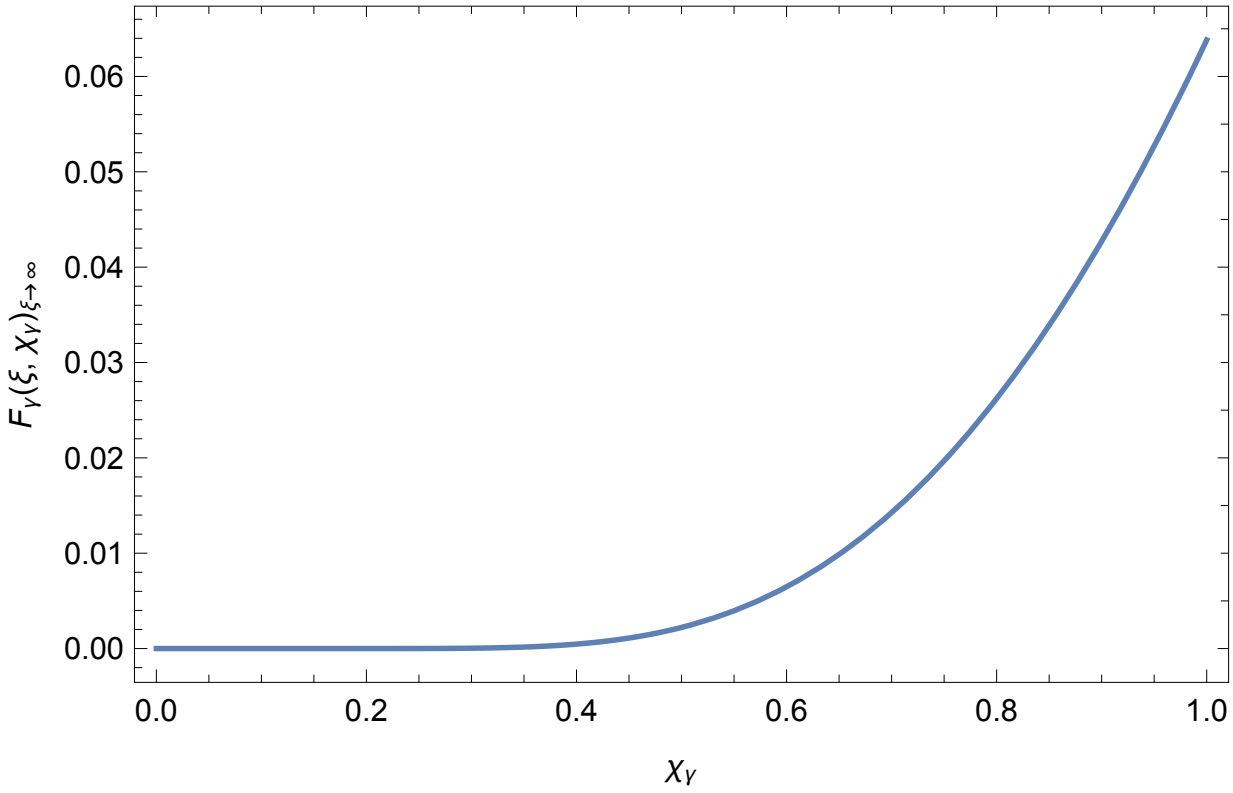

Figure 2.10: Limiting value $\xi >> 1$ of pair-production probability as a function of χ_γ. As the parameter χ_γ is responsible of the magnitude for the nonlinearities effects, for $\xi >> 1$ it is seen that these effects are optimal for $\chi_\gamma \sim 1$ even when asymptotic results are only valid for $\chi_\gamma << 1$

Higher order terms contribute to larger ξ and n and the loss of terms with small n becomes unnoticeable. If we focus on Figure 2.10, the dependency on ξ for small χ_γ is acutely non monotonic. After some convenient ratio, the probability maxima become of the same order and the monotonic nature of the curve gets smoothed out. Figure 2.10 shows the limiting value

of the probability for $\xi \sim \infty$. This limit have a tremendous impact when the behaviour observed is in the non perturbative regime, the most important contribution comes from the limit $\chi_e \sim 1$, even when the asymptotic expression is only valid when this parameter is smaller than one.

Conclusions

In the present thesis, there has been discussed two projects that were part of this PhD thesis. The first of them was the correction to the dark fermion magnetic moment [15] and the second the computation for the rates of electron positron pair production near the non perturbative Schwinger regime [34]. Conclusions for both problems are listed below. Also during the thesis, articles were named, which have not been discussed here and in which have also been part of this thesis project. They have been added as an appendix at the end of this work.

Dark Matter and Kinetic Mixing: Anomalous Magnetic Moment of a Dark QED Fermion

For a model of Dark Matter quantum electrodynamics, coupled to a visible photon it was computed the anomalous magnetic moment of the dark fermion. The coupling to visible matter is by mean of a kinetic mixing term, which connects the dark and visible sector of the universe. In correspondence to QED, a dark QED fermion should have a gyromagnetic factor g_Ψ

related to the correction of the magnetic moment.

In this case there are two contributions for the form factor in which the gyromagnetic factor value is hidden. It has been found that in a case in which only dark matter is involved in the process and the case in which the dark matter vertex includes an external visible photon are related by means of the form factor and only differ by a constant associated to the order of interaction for the kinetic mixing parameter.

An expression as been found for the gyromagnetic factor g_Ψ for the case in which a visible photon interacts with a dark fermion and the vertex has a dark virtual photon in the loop and in the case in which the external photon is dark g'_Ψ.

Measuring the boiling point of vacuum of quantum electrodynamics

The rate of electron positron pair production in a Bremsstrahlung Spectrum has been computed, considering the new set-up to use at the LUXE experiment at DESY (see Figure 2.1). It has been found that the rates corresponding to Spontaneous Pair Production and Bremsstrahlung laser-assisted one photon pair production in the limit of for $\xi \gtrsim \frac{1}{\sqrt{\chi_e}} \gg 1$ are closely related:

$$\frac{\Gamma_{\mathrm{SPP}}}{V} = \frac{m_e^4}{(2\pi)^3}\left(\frac{|E|}{E_c}\right)^2 \sum_{n=1}^{\infty} \frac{1}{n^2} \exp\left(-n\pi \frac{E_c}{|E|}\right)$$

$$\Gamma_{\mathrm{BPPP}} \to \frac{9}{128}\sqrt{\frac{3}{2}}\,\alpha\,E_e\,(1+\cos\theta)^2\left(\frac{|\mathbf{E}|}{E_c}\right)^2 \exp\left[-\frac{8}{3}\frac{1}{1+\cos\theta}\frac{m_e}{\omega_i}\frac{E_c}{|\mathbf{E}|}\right].$$

Even though there is a small range of parameters in where the asymptotic approximation holds, the number of pair expected to be produced is favourably high, enough to be measured with the present technology and it should be possible to measure the Schwinger critical field in this kind of experiment.

One pair at least should be measured around an intensity above $3 \times 10^{18}\frac{\mathrm{W}}{\mathrm{cm}^2}$, which is below the range described above. The perturbative regime starts at $5 \times 10^{18}\frac{\mathrm{W}}{\mathrm{cm}^2}$, for the parameters that will take place at the LUXE experiment.

The behaviour of the rate in terms of the intensity and also on the value of E_c shows, that a slight variation of the 10% on the last one would affect the rate in approximately one order of magnitude with this difference being smaller for higher intensities.

Bibliography

[1] P. Arias, A. K. Das, J. Gamboa, and F. Mendez. Generalized Dirac duality and CP violation in a two photon theory. *Mod. Phys. Lett.*, A32(05):1750032, 2017.

[2] P. Arias, J. Gamboa, and N. Tapia. Anapole Dark Matter Interactions as Soft Hidden Photons. *Phys. Lett.*, B791:17–19, 2019.

[3] N. Arkani-Hamed, D. P. Finkbeiner, T. R. Slatyer, and N. Weiner. A Theory of Dark Matter. *Phys. Rev.*, D79:015014, 2009.

[4] A. Arza, J. Gamboa, and N. Tapia. Photons and Dark Photons Through Breit-Wheeler Processes. *arXiv:1612.09187*, 2016.

[5] C. Bamber et al. Studies of nonlinear QED in collisions of 46.6-GeV electrons with intense laser pulses. *Phys. Rev.*, D60:092004, 1999.

[6] V. Barger, W.-Y. Keung, and D. Marfatia. Electromagnetic properties of dark matter: Dipole moments and charge form factor. *Phys. Lett.*, B696:74–78, 2011.

[7] L. Bergstrom and A. Goobar. *Cosmology and particle astrophysics*. Berlin, Germany: Springer (2004) 364 p, 1999.

[8] C. A. Bertulani. *Nuclear physics in a nutshell*, volume 2. Princeton University Press, 2007.

[9] T. G. Blackburn and M. Marklund. Nonlinear Breit-Wheeler pair creation with bremsstrahlung γ rays. *Plasma Phys. Control. Fusion*, 60: 054009, 2018.

[10] H. Bondi. Negative mass in general relativity. *Rev. Mod. Phys.*, 29:423–428, Jul 1957. URL `https://link.aps.org/doi/10.1103/RevModPhys.29.423`.

[11] F. Brummer and J. Jaeckel. Minicharges and Magnetic Monopoles. *Phys. Lett.*, B675:360–364, 2009.

[12] F. Brummer, J. Jaeckel, and V. V. Khoze. Magnetic Mixing: Electric Minicharges from Magnetic Monopoles. *JHEP*, 06:037, 2009.

[13] C. Bula, K. T. McDonald, E. J. Prebys, C. Bamber, S. Boege, T. Kotseroglou, A. C. Melissinos, D. D. Meyerhofer, W. Ragg, D. L. Burke, R. C. Field, G. Horton-Smith, A. C. Odian, J. E. Spencer, D. Walz, S. C. Berridge, W. M. Bugg, K. Shmakov, and A. W. Weidemann. Observation of nonlinear effects in compton scattering. *Phys. Rev. Lett.*, 76:3116–3119, Apr 1996. URL `https://link.aps.org/doi/10.1103/PhysRevLett.76.3116`.

[14] D. L. Burke, R. C. Field, G. Horton-Smith, J. E. Spencer, D. Walz, S. C. Berridge, W. M. Bugg, K. Shmakov, A. W. Weidemann, C. Bula, K. T. McDonald, E. J. Prebys, C. Bamber, S. J. Boege, T. Koffas, T. Kotseroglou, A. C. Melissinos, D. D. Meyerhofer, D. A. Reis, and W. Ragg. Positron production in multiphoton light-by-light scattering. *Phys. Rev. Lett.*, 79:1626–1629, Sep 1997. URL `https://link.aps.org/doi/10.1103/PhysRevLett.79.1626`.

[15] A. K. Das, J. Gamboa, F. Mndez, and N. Tapia. Testing dark matter with the anomalous magnetic moment in a dark matter quantum electrodynamics model. *Mod. Phys. Lett.*, A32(33):1750175, 2017.

[16] A. Di Piazza. Ultrarelativistic electron states in a general background electromagnetic field. *Phys. Rev. Lett.*, 113:040402, Jul 2014. URL `https://link.aps.org/doi/10.1103/PhysRevLett.113.040402`.

[17] A. Di Piazza. Analytical tools for investigating strong-field qed processes in tightly focused laser fields. *Phys. Rev. A*, 91:042118, Apr 2015. URL `https://link.aps.org/doi/10.1103/PhysRevA.91.042118`.

[18] A. Di Piazza. Nonlinear breit-wheeler pair production in a tightly focused laser beam. *Phys. Rev. Lett.*, 117:213201, Nov 2016. URL `https://link.aps.org/doi/10.1103/PhysRevLett.117.213201`.

[19] A. Di Piazza. First-order strong-field qed processes in a tightly focused laser beam. *Phys. Rev. A*, 95:032121, Mar 2017. URL https://link.aps.org/doi/10.1103/PhysRevA.95.032121.

[20] A. D. Dolgov and Ya. B. Zeldovich. Cosmology and Elementary Particles. *Rev. Mod. Phys.*, 53:1–41, 1981.

[21] F. Donato. Indirect searches for dark matter. *Phys. Dark Univ.*, 4: 41–43, 2014.

[22] D. Ehrenstein. Conjuring matter from light. *Science*, 277(5330): 1202, 1997. ISSN 0036-8075. URL http://science.sciencemag.org/content/277/5330/1202.

[23] ELI-laser. Science Applications: High fields, 2017. URL https://eli-laser.eu/science-applications/high-fields-physics/. Accessed: 2019-07-15.

[24] A. Erdelyi. Asymptotic expansions. *Dover Publications*, 2010.

[25] H. Falomir, J. Gamboa, and F. Mendez. Non-Abelian Monopoles as the Origin of Dark Matter. *Mod. Phys. Lett.*, A31(24):1650136, 2016.

[26] Farnes, J. S. A unifying theory of dark energy and dark matter: Negative masses and matter creation within a modified framework. *A&A*, 620:A92, 2018. URL https://doi.org/10.1051/0004-6361/201832898.

[27] J. Gamboa and F. Mendez. Dark and Visible Photons as Source of CP Violation. *ARXIV:1506.05042*, 2015.

[28] S. Gardner. Shedding light on dark matter: A faraday rotation experiment to limit a dark magnetic moment. *Phys. Rev. D*, 79:055007, Mar 2009. URL https://link.aps.org/doi/10.1103/PhysRevD.79.055007.

[29] R. Garner. *Fermi Data Tantalize With New Clues To Dark Matter*. 2015.

[30] G. B. Gelmini. TASI 2014 Lectures: The Hunt for Dark Matter. In *Theoretical Advanced Study Institute in Elementary Particle Physics: Journeys Through the Precision Frontier: Amplitudes for Colliders (TASI 2014) Boulder, Colorado, June 2-27, 2014*, 2015. URL http://inspirehep.net/record/1342951/files/arXiv:1502.01320.pdf.

[31] D. Goldberg. *The standard model in a nutshell*, volume 18. Princeton University Press, 2017.

[32] W. Greiner and J. Reinhardt. *Quantum electrodynamics*. Berlin, Germany: Springer (1992) 308 p., 1992. ISBN 9783540875604.

[33] P.-H. Gu. Multi-component dark matter with magnetic moments for fermi-lat gamma-ray line. *Physics of the Dark Universe*, 2(1):35 – 40, 2013. ISSN 2212-6864. URL http://www.sciencedirect.com/science/article/pii/S2212686413000058.

[34] A. Hartin, A. Ringwald, and N. Tapia. Measuring the boiling point of the vacuum of quantum electrodynamics. *Phys. Rev. D*, 99:036008, Feb 2019. URL https://link.aps.org/doi/10.1103/PhysRevD.99.036008.

[35] C. Harvey, T. Heinzl, and A. Ilderton. Signatures of High-Intensity Compton Scattering. *Phys. Rev.*, A79:063407, 2009.

[36] J. G. Heinrich, C. Lu, K. T. McDonald, C. Bamber, A. C. Melissinos, D. Meyerhofer, Y. Semertzidis, P. Chen, J. Spencer, and R. B. Palmer. Proposal for a study of QED at critical field strength in intense laser high-energy electron collisions at the Stanford Linear Accelerator. 1991.

[37] B. Holdom. Two U(1)'s and Epsilon Charge Shifts. *Phys. Lett.*, B166: 196–198, 1986.

[38] C. Itzykson and J. B. Zuber. *Quantum Field Theory*. International Series In Pure and Applied Physics. McGraw-Hill, New York, 1980. ISBN 9780486445687, 0486445682. URL http://dx.doi.org/10.1063/1.2916419.

[39] E. W. Kolb and M. S. Turner. The Early Universe. *Front. Phys.*, 69: 1–547, 1990.

[40] C. Kouvaris, K. Langæble, and N. G. Nielsen. The spectrum of darkonium in the sun. *Journal of Cosmology and Astroparticle Physics*, 2016

(10):012, oct 2016. URL https://doi.org/10.1088%2F1475-7516%2F2016%2F10%2F012.

[41] B. Kumar, M. B. Paranjape, and U. A. Yajnik. Fate of the false monopoles: Induced vacuum decay. *Phys. Rev.*, D82:025022, 2010.

[42] P. Langacker. *The standard model and beyond.* Boca Raton, USA: CRC Pr. (2010) 663 p, 2010. ISBN 9781420079067. URL http://www.taylorandfrancis.com/shopping_cart/search/search.asp?search=978-1-4200-7906-7.

[43] M. Lisanti. Lectures on Dark Matter Physics. In *Theoretical Advanced Study Institute in Elementary Particle Physics: New Frontiers in Fields and Strings (TASI 2015) Boulder, CO, USA, June 1-26, 2015*, 2016. URL http://inspirehep.net/record/1427360/files/arXiv:1603.03797.pdf.

[44] J. Luttinger. On ?negative? mass in the theory of gravitation. *Awards for Essays on Gravitation,(Gravity Research Foundation, 1951)*, 1951.

[45] R. Mann. Black holes of negative mass. *Classical and Quantum Gravity*, 14(10):2927–2930, oct 1997. URL https://doi.org/10.1088%2F0264-9381%2F14%2F10%2F018.

[46] S. Mbarek and M. B. Paranjape. Negative mass bubbles in de sitter spacetime. *Phys. Rev. D*, 90:101502, Nov 2014. URL https://link.aps.org/doi/10.1103/PhysRevD.90.101502.

[47] K. T. McDonald. Fundamental physics during violent accelerations. *AIP Conf. Proc.*, 130:23–54, 1985.

[48] V. Mukhanov. *Physical Foundations of Cosmology*. Cambridge University Press, Oxford, 2005. ISBN 0521563984, 9780521563987. URL http://www-spires.fnal.gov/spires/find/books/www?cl=QB981.M89::2005.

[49] N. Narozhny, S. Bulanov, V. Mur, and V. Popov. e+e-pair production by a focused laser pulse in vacuum. *Physics Letters A*, 330(1):1 – 6, 2004. ISSN 0375-9601. URL http://www.sciencedirect.com/science/article/pii/S0375960104009971.

[50] N. Narozhnyi, A. Nikishov, and V. Ritus. Quantum processes in the field of a circularly polarized electromagnetic wave. *Zh. Eksperim. i Teor. Fiz.*

[51] E. National Academies of Sciences and Medicine. *Opportunities in Intense Ultrafast Lasers: Reaching for the Brightest Light*. The National Academies Press, Washington, DC, 2018. ISBN 978-0-309-46769-8. URL https://www.nap.edu/catalog/24939/opportunities-in-intense-ultrafast-lasers-reaching-for-the/-brightest-light.

[52] A. I. Nikishov and V. I. Ritus. Quantum Processes in the Field of a Plane Electromagnetic Wave and in a Constant Field 1. *Sov. Phys. JETP*, 19:529–541, 1964. [Zh. Eksp. Teor. Fiz.46,776(1964)].

[53] A. I. Nikishov and V. I. Ritus. Quantum Processes in the Field of a Plane Electromagnetic Wave and in a Constant Field 2. *Sov. Phys. JETP*, 19:1191–1199, 1964. [Zh. Eksp. Teor. Fiz.46,1768(1964)].

[54] P. J. E. Peebles. *Principles of physical cosmology*. Princeton, USA: Univ. Pr. (1993) 718 p, 1994.

[55] M. E. Peskin and D. V. Schroeder. *An Introduction to quantum field theory*. Reading, USA: Addison-Wesley (1995) 842 p, 1995. ISBN 9780201503975, 0201503972. URL `http://www.slac.stanford.edu/spires/find/books/www?cl=QC174.45%3AP4`.

[56] M. Pospelov and T. ter Veldhuis. Direct and indirect limits on the electromagnetic form-factors of WIMPs. *Phys. Lett.*, B480:181–186, 2000.

[57] F. Reddy. NASA's Fermi Mission Expands its Search for Dark Matter, 2016.

[58] V. I. Ritus. Quantum effects of the interaction of elementary particles with an intense electromagnetic field. *Journal of Soviet Laser Research*, 6(5):497–617, Sep 01, 1985. ISSN 1573-8760. URL `https://doi.org/10.1007/BF01120220`.

[59] M. D. Schwartz. *Quantum Field Theory and the Standard Model*. Cambridge University Press, 2014. ISBN 1107034736, 9781107034730. URL http://www.cambridge.org/us/academic/subjects/physics/theoretical-physics-and-mathematical-physics/quantum-field-theory-and-standard-model.

[60] SLAC-E144. SLAC Experiment 144 Home Page, 1985. URL https://www.slac.stanford.edu/exp/e144/e144.html#About\%20the\%20Experiment. Accessed: 2018-09-19.

[61] C. G. Tully. *Elementary particle physics in a nutshell*. Princeton, USA: Univ. Pr. (2011) 303 p, 2011.

[62] M. Visser and D. L. Wiltshire. Stable gravastarsan alternative to black holes? *Classical and Quantum Gravity*, 21(4):1135, 2004. URL http://stacks.iop.org/0264-9381/21/i=4/a=027.

[63] A. Zee. *Quantum field theory in a nutshell*. Princeton, UK: Princeton Univ. Pr. (2010) 576 p, 2003. ISBN 0691140340, 9780691140346.

[64] F. Zwicky. On the Masses of Nebulae and of Clusters of Nebulae. *Astrophys. J.*, 86:217–246, 1937.

Appendix A

Negative mass bubbles

Introduction

The Schwarzschild solution is an exact vacuum solution of the Einstein equations which contains the mass as the only free parameter. The solution has a singularity at Schwarzschild coordinate $r = 0$, which is called a black hole, for a positive mass, and the singularity is hidden behind a null surface called the event horizon. If an observer stays outside the event horizon, he is safe from the singularity. However, if he crosses over the null surface and enters the black hole he cannot avoid the singularity and in finite time he is ripped apart by the infinite gravitational stresses that occur at this point. On the other hand, for a negative mass, the singularity is naked as it has no event horizon covering it [45]. However, it is point like, and occurs at a fixed spatial position. An observer can view the singularity from a distance, and in principle, every observer who chooses not to impinge on the singularity can

avoid it forever. Indeed, the singularity of the negative mass Schwarzschild solution appears to be relatively benign compared to the one of a positive mass. The most basic example of this kind of singularity would be a point charge in the case of electrodynamics

The corresponding electric field is in principle, singular at the location of the point charge, and the total energy is infinite. From a large distance, a singular point charge is harmless, we can simply avoid it, and at close distance we expect that the singular nature of the charge will be smoothed out by a concentrated but non-singular charge density. The analogous situation in the context of general relativity and the negative mass Schwarzschild solution, is to ask if there is a non-singular distribution of energy momentum density that smooths out its singularity.

The idea of this study is to find a configuration in which the mass of the bubbles would be negative, seen from the outside, in a Schwarzschild de-Sitter space, having into account the dominant energy condition and the stability of the bubble. The dominant energy condition is equivalent to the statement that no Lorentz observer can see the energy momentum to be moving out of the future directed light cone. It has been established [41] that the possibility of non-singular negative mass configurations could exist that correspond to physically reasonable energy-momentum. In a following article, [46] it was shown that with energy and momentum given by a ideal fluid, there exist bubble like configurations which exterior to the bubble correspond exactly to the negative mass Schwarzschild-de Sitter space-time. Negative mass objects would be exotic matter and would exhibit new phe-

nomena [44]. As Luttinger stablished on his prize winning essay "One negative mass", negative mass objects would gravitationally repel all objects of any mass (positive or negative), while positive mass objects, regular matter would gravitationally attract all objects of any mass, as we usually define it. A negative mass object will follow a positive mass object and they would move in the same direction, among some other interesting behaviour.

Details

The energy momentum tensor of a perfect fluid, considering the cosmological constant would be

$$T^{\mu\nu} = (\rho + P)U^{\mu}U^{\nu} + Pg^{\mu\nu} + \Lambda g^{\mu\nu}. \tag{A.1}$$

If this is plug into the Einstein'a field equation

$$R_{\mu\nu} = \kappa \left(T_{\mu\nu} - \frac{1}{2} g_{\mu\nu} T \right), \tag{A.2}$$

where $\kappa = 8\pi G$. With $T = -\rho + 3P$ so

$$R_{\mu\nu} = \kappa \left[(\rho + P)U^{\mu}U^{\nu} + \frac{1}{2}(\rho - P)g_{\mu\nu} \right] + \Lambda g^{\mu\nu}. \tag{A.3}$$

If we assume a static spherically symmetric interior described by the metric

$$ds^2 = -A(r)dt^2 + B(r)dr^2 + r^2 d\Omega^2 \tag{A.4}$$

The field equation implies

$$R_{tt} = \frac{A''}{2B} + \frac{A'}{rB} - \frac{A'}{4B}\left(\frac{A'}{A} + \frac{B'}{B}\right) = \left[\frac{1}{2}\kappa(\rho + 3P) + \Lambda\right] A \quad \text{(A.5)}$$

$$R_{rr} = -\frac{A''}{2A} + \frac{B'}{rB} - \frac{A'}{4A}\left(\frac{A'}{A} + \frac{B'}{B}\right) = \left[\frac{1}{2}\kappa(\rho - P) - \Lambda\right] B \quad \text{(A.6)}$$

$$R_{rr} = 1 + \frac{1}{B} - \frac{r}{2B}\left(\frac{A'}{A} - \frac{B'}{B}\right) = \left[\frac{1}{2}\kappa(\rho - P) - \Lambda\right] r^2. \quad \text{(A.7)}$$

To get rid of the second derivative the next combination is useful

$$\frac{R_{tt}}{A} + \frac{R_{rr}}{B} + 2\frac{R_{\theta\theta}}{r^2} = \left(\frac{2}{r^2} - \frac{2}{r^2 B} + \frac{2B'}{rB^2}\right) = 2(\kappa\rho + \Lambda). \quad \text{(A.8)}$$

From here we find that for B

$$B = \left(1 - \frac{2m(r) + \Lambda r^3/3}{r}\right)^{-1}, \quad \text{(A.9)}$$

considering the next definition for the mass $m(r) = \int_0^r \frac{\kappa}{2}\rho(r')r'^2 dr'$. An equation for A can be found in a similar way, using $\frac{R_{tt}}{A} + \frac{R_{rr}}{B} - 2\frac{R_{\theta\theta}}{r^2}$, which gives

$$\frac{1}{rB}\frac{A'}{A} - \frac{1}{r^2} + \frac{1}{r^2 B} = (P\kappa - \Lambda) \quad \text{(A.10)}$$

and can also be written as

$$\frac{A'}{A} = \frac{B}{r^2}\left(2m(r) + \left(P\kappa - \frac{2}{3}\Lambda\right) r^3\right). \quad \text{(A.11)}$$

The condition for hydrostatic equilibrium on the pressure gradient $P' = \frac{dP}{dr}$, which together with the equation for the field A lead us to the Tolman-Oppenheimer-Volkoff (TOV) equation

$$P' = -\frac{m(r)\rho(r)}{r^2}\left(1+\frac{\left(\frac{P\kappa}{2}-\frac{2\Lambda}{3}\right)r^3}{m(r)}\right)\left(1+\frac{P}{\rho(r)}\right)\left(1-\frac{2m(r)+\Lambda r^3/3}{r}\right)^{-1}. \tag{A.12}$$

The dominant energy condition ($\rho \geq |P|$) allow us to simplify the TOV equation, neglecting a factor

$$P' = -\frac{m(r)\rho(r)}{r^2}\left(1+\frac{\left(\frac{P\kappa}{2}-\frac{2\Lambda}{3}\right)r^3}{m(r)}\right)\left(1-\frac{2m(r)+\Lambda r^3/3}{r}\right)^{-1}. \tag{A.13}$$

In this case we look to the case in which the fluid is the Chaplygin gas whose equation of state is

$$P = -\frac{C}{\rho} \tag{A.14}$$

This give rise to the following system of first-order differential equations for P and M

$$\frac{dP}{dr} = \frac{m(r)C}{r^2P}\left(1+\frac{\left(\frac{\kappa P}{2}-\frac{2\Lambda}{3}\right)r^3}{m(r)}\right)\left(1-\frac{2m(r)+\Lambda r^3/3}{r}\right)^{-1}. \tag{A.15}$$

$$\frac{dm(r)}{dr} = -\frac{\kappa}{2}\frac{Cr^2}{P}, \tag{A.16}$$

which is an interesting case for further studies. Generally this election is related to dark energy.

The junction condition

The balance of the energy momentum flux through the interface gives rise to what are called the Israel junction conditions

$$(1 - 2m(r)/r - \frac{\Lambda_i r^2}{3} + \dot{r}^2)^{1/2} - (1 - 2M/r - \frac{\Lambda_e r^2}{3} + \dot{r}^2)^{1/2} = 4\pi\sigma r \tag{A.17}$$

Squaring twice and rearranging the terms

$$\begin{aligned}\dot{r}^2 &= \frac{1}{576\pi^2 r^4\sigma^2}\Big[12m(r)\left(3m(r) - 6M + r^3\left(-\Lambda\mathrm{e} + \Lambda\mathrm{i} + 48\pi^2\sigma^2\right)\right) \\ &+ 96\pi^2 r^3\sigma^2\left(6M + r^3(\Lambda\mathrm{e} + \Lambda\mathrm{i}) - 6r\right) + \left(6M + r^3(\Lambda\mathrm{e} - \Lambda\mathrm{i})\right)^2 + 2304\pi^4 r^6\sigma^4\Big]\end{aligned}$$

Wich can also be written in the next way, considering that $V(r) + \frac{1}{2}\dot{r} = E$ and we expect a completely stable solution which correspond to $E = 0$, thus

$$V(r) = -\frac{\alpha}{r^4} - \frac{\beta}{r} - \gamma r^2 + \frac{1}{2} \tag{A.18}$$

with

$$
\begin{aligned}
\alpha &= \frac{1}{32\pi^2\sigma^2}\left(m(r)-M\right)^2, \\
\beta &= \frac{1}{96\pi^2\sigma^2}\left[\left(\Lambda_e-\Lambda_i\right)\left(M-m(r)\right)\right]+\frac{m(r)+M}{2}, \\
\gamma &= \frac{1}{1152\pi^2\sigma^2}\left(\Lambda_e-\Lambda_i\right)^2+\frac{\Lambda_e+\Lambda_i}{12}+2\pi^2\sigma^2
\end{aligned}
$$

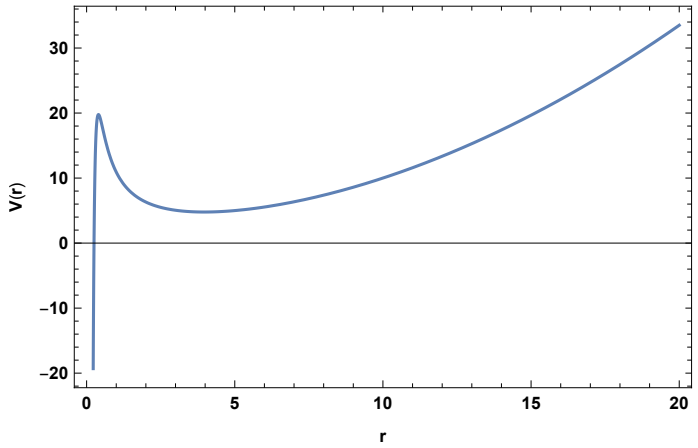

Figure A.1: For parameters $\alpha = 0.16, \beta = -10., \gamma = -0.08$ the function V(r). It can be seen that the potential has a local minimum, not stable and we need higher orders in the potential to modulate the behaviour of the bubble.

The second junction condition correspond to

$$
8\pi\vartheta r = \frac{1-\frac{m(r)}{r}-\frac{2\Lambda_i r^2}{3}-m'(r)+r\ddot{r}}{\sqrt{1-\frac{2m(r)}{r}-\frac{\Lambda_i r^2}{3}+\dot{r}^2}}-\frac{1-\frac{M}{r}-\frac{2\Lambda_e r^2}{3}+r\ddot{r}}{\sqrt{1-\frac{2M}{r}-\frac{\Lambda_e r^2}{3}+\dot{r}^2}} \tag{A.19}
$$

In this sense we found a dynamic expression for the radius of the bubble, but in order to completely specify its stability we need to now $m(r)$, and this give us infinite possibilities, to find a minimum in the potential. We look a way to restrict the mas seen from the outside of the bubble, by specifying that it has to go to zero near the origin and the dominant energy conditions.

Dynamic master equation

According to [62] the dynamic 'master equation 'can be written terms of the masses of the problem, being $m_+(a) = -M + \lambda a^3/6$ the mass exterior to the radius a, $m_s(a) = 4\pi\sigma a^2$ the mass of the shell itself and $m_-(a)$ the mass inside the radius a, being a the surface of the bubble.

In this case the potential has the form

$$V(a) = \frac{1}{2}\left(- \left(\frac{(m_-(a) + m_+(a))}{m_s(a)} + \frac{m_s(a)}{(2a)} \right)^2 + \left(4\frac{m_-(a)m_+(a)}{m_s(a)^2} \right) + 1 \right), \tag{A.20}$$

and is a consequence of the junction condition.

If we impose a potential having a minimum we can find the corresponding $m_-(a)$ for this potential. Solving for the mas $m_-(a)$ then it is found that

$$m_-(a) = \mp \frac{\mathrm{m}_s(a)\sqrt{-2\mathrm{m}_+(a) - 2a\mathrm{V}(a) + a}}{\sqrt{a}} + \mathrm{m}_+(a) - \frac{\mathrm{m}_s(a)^2}{2a} \tag{A.21}$$

The mass near the center is expected to be zero, and for that the potential near zero can be found to fulfil this condition. Only the positive root for $m_{-}(a)$ will make the potential force the mass to go to zero at $a = 0$. The shape of the potential **near** zero would be

$$V(a) = \frac{1}{2}\left(1 + \frac{2M}{a} - \frac{M^2}{m_s(a)^2}\right), \tag{A.22}$$

and away from zero could have higher powers of a that would respect the shape near zero.

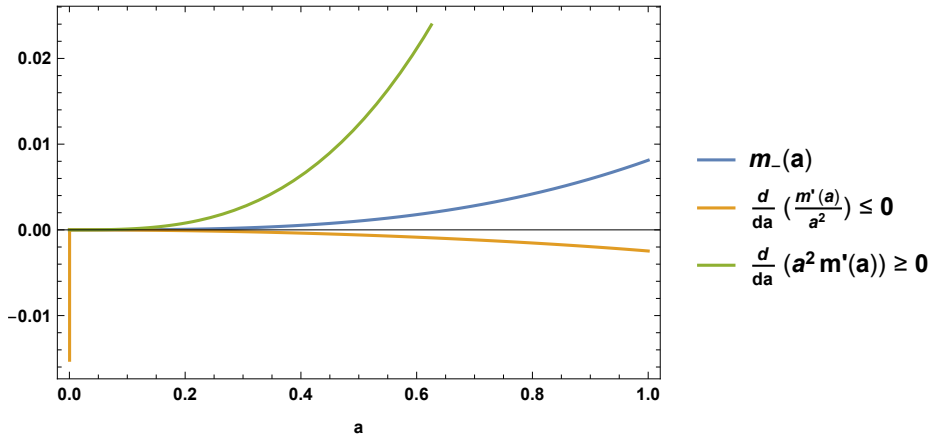

Figure A.2: The dominant energy conditions for the mass of the bubble, for parameters $\{M = 0.01, \Lambda = 0.001, \sigma = 0.001\}$

So we look for a potential of the shape

$$V_{a\to 0}(a) = \frac{\alpha}{a^4} + \frac{\beta}{a} + \gamma a^2 + \frac{1}{2} \tag{A.23}$$

and that will also fulfil the dominant energy condition. The dominant energy condition is equivalent to the next two inequalities,

$$\frac{d}{da}\left(\frac{m'(a)}{a^2}\right) \leq 0 \tag{A.24}$$

$$\frac{d}{da}\left(m'(a)a^2\right) \geq 0 \tag{A.25}$$

When this potential $V_{a\to 0}(a)$ is inserted in $m_{-}(a)$ it fulfils the conditions above for $a \to 0$. It is clear from Figure A.2 that higher powers are needed to have a minima and fulfil the dominant energy conditions.

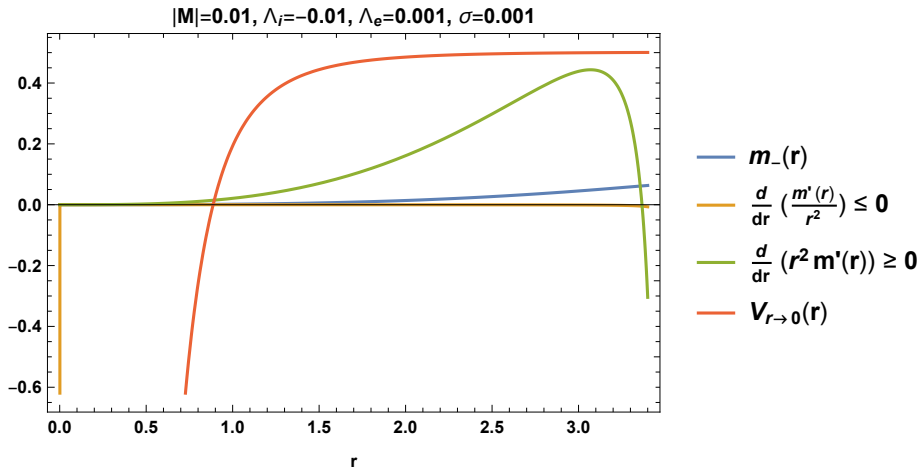

Figure A.3: Dominant energy conditions, for parameters $\{M = 0.01, \Lambda_i = 0.001, \Lambda_e = 0.001, \sigma = 0.001\}$

If we check the conditions mentioned above, that is the stability for the potential and the dominant energy conditions, we find that there is no minimum for the potential in the range in which the stability and energy

conditions are fulfilled, as we can see in Figure A.3. The mass (blue) is positive and goes to zero near the origin, the dominant energy conditions are satisfied but the potential has no minimum and that means that the solution is not stable.

As we can see in the previous figure, it is necessary to add higher order terms that will not contribute to the potential near the origin but that could make a minimum further.

Stable negative mass solutions

It can be understood from the previous section that we need a potential that approaches zero with a power r^{-4}. If we take again $m_{-}(a)$ in eq. (A.21) and clear $V(a)$ for it we get, now in terms of r

$$m_{-}(r) = -8\pi^2\sigma^2 r^3 + -M + \frac{\Lambda r^3}{6} + 4\pi\sigma r^2\sqrt{1 - 2V(r) - \frac{2M}{r} - \frac{\Lambda r^2}{3}}. \quad \text{(A.26)}$$

The leading order contribution from the square root near zero is the r^{-4} term. So we take a potential with the shape

$$-2V(r) = \frac{1 + \tilde{V}(r)}{\sigma^2 r^4} \quad \text{(A.27)}$$

it is found for the mass equation that

$$m_{-}(r) = M\left[-1 + \frac{1}{2}\left(\Lambda - \sigma^2\right) r^3 + \sqrt{1 + \tilde{V}(r) + \sigma^2 r^4 + 2\sigma^2 r^3 - \Lambda\sigma^2 r^6}\right]. \tag{A.28}$$

Now if we define a new function

$$(1 + U(r))^2 = 1 + \tilde{V}(r) + \sigma^2 r^4 + 2\sigma^2 r^3 - \Lambda\sigma^2 r^6 \tag{A.29}$$

and we get a simple expression for the mass

$$m_{-}(r) = M\left(\frac{1}{2}\left[\Lambda - \sigma^2\right] r^3 + U(r)\right) \tag{A.30}$$

Now, the dominant energy conditions can be refrased as

$$\frac{d}{dr}\left(\frac{m'_{-}(r)}{r^2}\right) \leq 0 \quad and \quad \frac{d}{dr}\left(m'_{-}(r) r^2\right) \geq 0 \tag{A.31}$$

and now we can write

$$\frac{d}{dr}\left(\frac{U'(r)}{r^2}\right) \leq 0 \quad and \quad 6\left[\Lambda - \sigma^2\right] + \frac{d}{dr}\left(U'(r) r^2\right) \geq 0. \tag{A.32}$$

Finally what is left it is, to choose $\tilde{V}(r)$ and $U(r)$ in such a way the they both fulfil the dominant energy conditions described above, that the mass is zero when it approximates the origin and that the potential $V(r)$ has a minimum at a certain r, where all these conditions are fulfilled. If this is the case then the bubble will have a dynamic equation with a stable configuration.

Appendix B

Articles

Photons and Dark Photons Through Breit-Wheeler Processes

Ariel Arza[a], Jorge Gamboa[a], and Natalia Tapia[a*]
[a] *Departamento de Física, Universidad de Santiago de Chile, Casilla 307, Santiago, Chile*

A variant of quantum electrodynamics coupled to a dark photon through a kinetic mixing is studied. The analogous of the light-light diagram becomes the conversion process $\gamma'\gamma' \to \gamma\gamma$ and an expression for the differential cross section is estimated. For high energies beams, as in LHC, this differential cross section could be measurable and its magnitude would be typically similar to the total cross section of neutrinos, *i.e.* $\sim 10^{-50}\,\mathrm{m}^2$.

* ariel.arza@usach.cl, jorge.gamboa@usach.cl, natalia.tapiaa@usach.cl

I. INTRODUCTION

One the most important challenges of particle physics in these days is to explain the origin, formation and dynamics of dark matter. Until now even though the existence of dark matter is well established result through the curves of rotation velocity of galaxies and formation of large structures, such as galactic halos and galaxy clusters. However, there are no other sufficiently robust sources corroborating its existence.

According to recent observations of the Fermi Gamma Ray Telescope [1] and others [2–6], an excess of photons is observed which can be explained, on the side, as a consequence of nearby pulsars or remnants of supernovas or, are simply processes of annihilation of dark matter processes in our galaxy.

In the latter context some explanations have been given, for example through the self-interacting dark matter models where the large effective cross section are explained, for example, through Sommerfeld enhancement [7, 8].

In this note we propose a mechanism that produces an excess of visible photon, which could be attributed to Breit-Wheeler process [9] in the sense is showed in the diagram

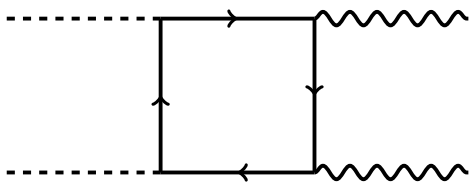

FIG. 1: This diagram corresponds to the $\gamma'\gamma' \to \gamma\gamma$ scattering where γ' are dark (hidden) photons and γ visible ones.

Formally this process can be seen as follows; if we cut the diagram as

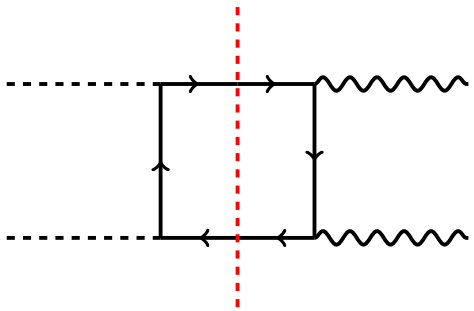

FIG. 2: Note that the *cut line* just describes two different physical processes, the left han side is a Breit-Wheeler ones and the right hand side is a pair annihilation.

then –in this mental image– one can see how the left hand side becomes a Breit-Wheeler process while the right hand side is just an annihilation one, however this *constructus* is theoretical and it is useful only to explain how dark photons could be converted to visible photons and viceversa. However in a general context, we need construct a framework where the vertices in FIG. 1 are reproduced and this is another of the goal of this letter.

II. THE FRAMEWORK

Physically, for visible photons, the annihilation and creation of pairs are related by

$$\sigma_c = 2|\mathbf{v}|^2\,\sigma_a, \tag{1}$$

where c and a denotes creation and annihilations of pairs respectively and $\mathbf{v}$ is the velocity of the pair. This formula was found by first time by Breit and Wheeler in 1934 although the Breit-Wheeler process $\gamma\gamma \to e^-e^+$ up to now remain as a non-observed prediction of QED.

The Breit-Wheeler process is much more difficult to produce than annihilation of pairs one. One can note that the equality between cross sections for Breit-Wheeler processes and annihilation pairs could be roughly similar only for extremely energetic massive particles. In [10] a photon-photon collider was proposed for detecting Breit-Wheeler process using a high power laser, but so far, there are no conclusive results.

Basically in a real processes one need to compute the total cross section

$$\sigma_{\text{total}} = \sigma\left(\gamma'\gamma' \to e^+e^- \to \gamma\gamma\right), \tag{2}$$

and this formula must show how dark photons are converted in visible ones and the calculation of this observable is another goal of this letter.

In order to implement our ideas let us consider the Lagrangean of QED

$$\mathcal{L}_{QED} = \bar{\psi}\left(i\partial\!\!\!/ + A\!\!\!/ - m\right)\psi - \frac{1}{4}F_{\mu\nu}(A)F^{\mu\nu}(A), \tag{3}$$

and we add the term

$$\mathcal{L}_{int} = -\frac{1}{4}F_{\mu\nu}(B)F^{\mu\nu}(B) + \frac{\xi}{2}F_{\mu\nu}(B)F^{\mu\nu}(A) + \frac{1}{2}m_\gamma^2 B_\mu B^\mu. \tag{4}$$

where we have added a term corresponding to the kinetic mixing term $F_{\mu\nu}(B)F^{\mu\nu}(A)$ introduced in [11] with B_μ a dark photon and m_γ the mass of this photon.

The total Lagrangean is

$$\mathcal{L}_{\text{total}} = \mathcal{L}_{QED} + \mathcal{L}_{int}. \tag{5}$$

In order to do tractable this Lagrangean is convenient to diagonalize A_μ by defining the transformation

$$A'_\mu = A_\mu - \xi\, B_\mu, \quad B'_\mu = B_\mu,$$

(5) becomes

$$\mathcal{L}_{total} = \bar{\psi}\left(i\partial\!\!\!/ + A\!\!\!/\,' + \xi\, B\!\!\!/ - m\right)\psi - \frac{(1-\xi^2)}{4}F_{\mu\nu}(A')F^{\mu\nu}(A') - \frac{1}{4}F_{\mu\nu}(B)F^{\mu\nu}(B) + \frac{1}{2}m_\gamma^2 B_\mu B^\mu, \tag{6}$$

and redefining the field A'_μ as $\sqrt{1-\xi^2}A'_\mu$ we have

$$\mathcal{L}_{total} = \bar{\psi}\left(i\partial\!\!\!/ + \frac{1}{\sqrt{1-\xi^2}}A\!\!\!/\,' + \xi\, B\!\!\!/ - m\right)\psi - \frac{1}{4}F_{\mu\nu}(A')F^{\mu\nu}(A') - \frac{1}{4}F_{\mu\nu}(B)F^{\mu\nu}(B) + \frac{1}{2}m_\gamma^2 B_\mu B^\mu, \tag{7}$$

but as $\xi << 1$, we can approximate $\frac{1}{\sqrt{1-\xi^2}} \approx 1$ and therefore (8) becomes

$$\mathcal{L}_{total} = \bar{\psi}\left(i\partial\!\!\!/ + A\!\!\!/ + \xi\, B\!\!\!/ - m\right)\psi - \frac{1}{4}F_{\mu\nu}(A)F^{\mu\nu}(A) - \frac{1}{4}F_{\mu\nu}(B)F^{\mu\nu}(B) + \frac{1}{2}m_\gamma^2 B_\mu B^\mu, \tag{8}$$

and the primes have been removed by simplicity.

Now we note that at fourth-order in perturbation theory the diagram FIG. 1 is reproduced where the vertices are $-i\gamma_\mu$ and $-i\,\xi\,\gamma_\mu$ for visible and dark photons respectively.

Taking this fact in mind, the differential cross section per unit solid angle Ω, in the limit of low energy, [12] for FIG. 1 is

$$\left.\frac{d\sigma(s,\theta)}{d\Omega}\right|_{\gamma'\gamma'\to e^-e^+\to\gamma\gamma} = \kappa\frac{\alpha^4\xi^4}{64\pi^2 m^8}s^3(3+\cos^2\theta)^2, \tag{9}$$

where $\alpha = e^2/4\pi$ is the fine structure constant, κ is a coefficient that depend of the explicit (difficult) calculation, but that is not important for this analysis and s is the Mandelstam variable

$$s = (p_1 + p_2)^2,$$

where $p_{1,2}$ are initial dark photons momenta.

In the center of mass frame, s can be written as

$$s = 4\left(\mathbf{p}^2 + m_\gamma^2\right) \equiv 4\,E^2,$$

with $E=\sqrt{\mathbf{p}^2+m_\gamma^2}$ the total energy of the dark photons.

Thus, we find

$$\left.\frac{d\sigma(E,\theta)}{d\Omega}\right|_{\gamma'\gamma'\to e^-e^+\to\gamma\gamma}=\kappa\frac{\alpha^4\xi^4}{\pi^2m^2}\left(\frac{E}{m}\right)^6(3+\cos^2\theta)^2. \tag{10}$$

For the high energy limit ($E\gg m$), we do not have an analytical expression for differential cross section such as (10), however it can be approached for $\theta=0$ and $\theta=\pi/2$. We have

$$\left.\frac{d\sigma(E,0)}{d\Omega}\right|_{\gamma'\gamma'\to e^-e^+\to\gamma\gamma}\sim\frac{\alpha^4\xi^4}{\pi^2m^2}\left(\frac{m}{E}\right)^2\left(\ln\frac{E}{m}\right)^4 \tag{11}$$

and

$$\left.\frac{d\sigma(E,\pi/2)}{d\Omega}\right|_{\gamma'\gamma'\to e^-e^+\to\gamma\gamma}\sim\frac{\alpha^4\xi^4}{\pi^2m^2}\left(\frac{m}{E}\right)^2. \tag{12}$$

Both cases (high and low energy limits) are very interesting because show how, in principle, dark photons could be transformed into visibles ones. It is also important to mention the process $\gamma'\gamma\to\gamma\gamma$ (see FIG. 3), where the initial photon can be prepared in the laboratory. In this case the formulas of differential cross sections should be scale as $d\sigma/d\Omega\sim\xi^2$. For instance, the high energy limit at $\theta=0$ is given by

$$\left.\frac{d\sigma(E,0)}{d\Omega}\right|_{\gamma'\gamma'\to e^-e^+\to\gamma\gamma}\sim\frac{\alpha^4\xi^2}{\pi^2m^2}\left(\frac{m}{E}\right)^2\left(\ln\frac{E}{m}\right)^4 \tag{13}$$

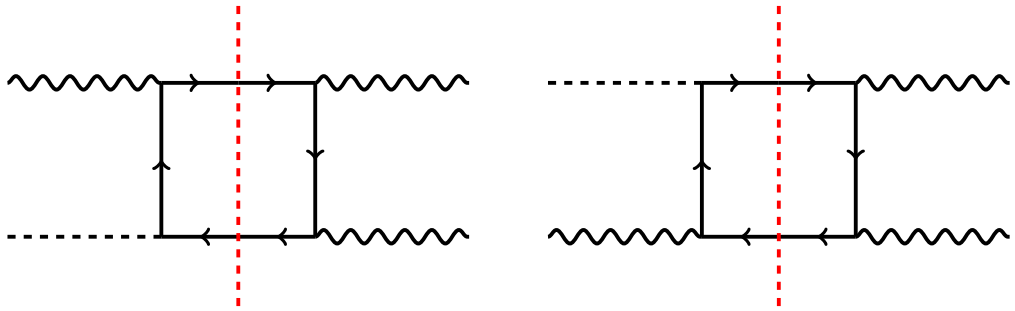

FIG. 3: This diagram corresponds to the $\gamma'\gamma'\to\gamma\gamma$ scattering where γ' are dark (hidden) photons and γ visible ones.

FIG. 4 shows, for the case $m_\gamma\gg|\mathbf{p}|$, the space of parameters (m_γ,ξ) where this process is allowed, taking into account typically like-neutrinos measurable cross sections [13].

Notice that below the black line and for masses $m_\gamma>10^6$ eV and $\xi>10^{-7}$, there is a window where differential cross sections of the order of $d\sigma/d\Omega\sim10^{-50}\,\mathrm{m}^2$ are allowed, which are typically values for neutrino-like particles. We found that this effect is sensitive in this unexplored space of parameters, where the masses m_γ are very large. Beyond these values, corrections of the standard model must be included.

III. COMMENTS AND CONCLUSION

There are several strategies aimed at detecting dark photons, for example using the bremsstrahlung where processes such as $e^-Z\to e^-ZA'$ where Z is nuclear target and A' is produced very forward and carrying the most of the beam energy, another example is the $e^-e^+\to\gamma A'$ where A' is a difference of energy which is attributed to dark photons and so on (these examples are explained in [14]).

In this paper we have considered a different route and we have proposed a mechanism where the basic process is a Breit-Wheeler one with two initial dark photons or one dark photon with a ordinary photon –including virtual processes– that convert this photons in visibles ones.

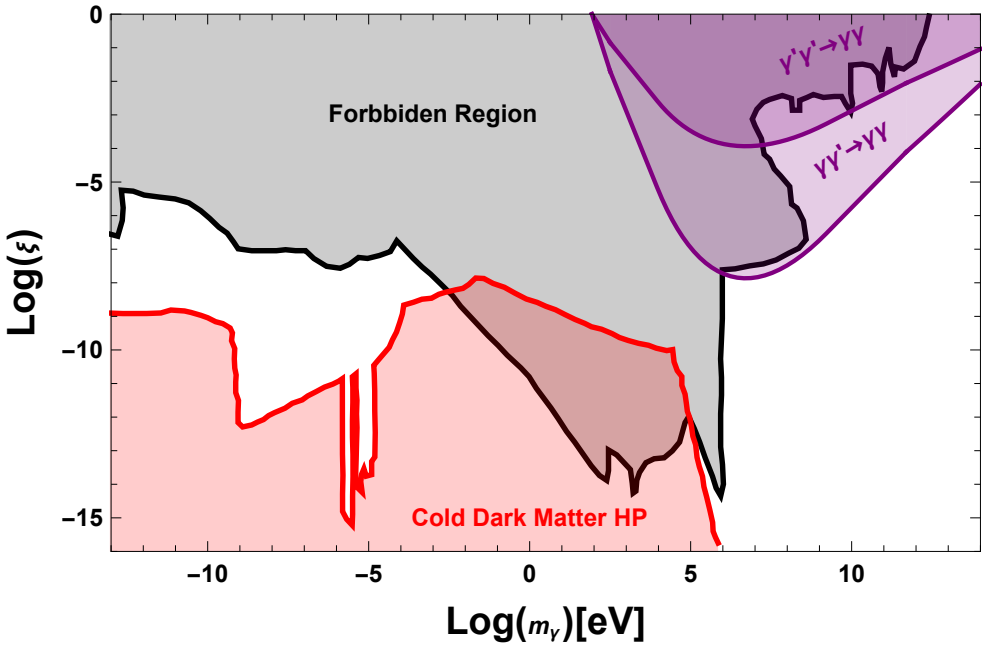

FIG. 4: This is an exclusion plot in search for hidden photons, the purple region is where the process studied is allowed for the processes $\gamma'\gamma' \to \gamma\gamma$ and $\gamma'\gamma \to \gamma\gamma$ with a differential cross section of $10^{-50}\mathrm{m}^2$ at $\theta = 0$. Gray region correspond to the excluded space and the pink region is where Hidden Photons can be cold dark matter.

Although Breit-Wheeler processes are still not observed even in conventional quantum electrodynamics, we can speculate with the orders of magnitude of possible cross sections. Indeed, the total cross section (11) can be written as

$$\begin{aligned} \left.\frac{d\sigma(E,0)}{d\Omega}\right|_{\gamma'\gamma'(\gamma)\to e^-e^+\to\gamma\gamma} &\sim \xi^{4(2)} \times \left(\tfrac{E}{m}\right)^6 \times 10^{-33}\mathrm{m}^2, \qquad E \ll m, \\ \left.\frac{d\sigma(E,0)}{d\Omega}\right|_{\gamma'\gamma'(\gamma)\to e^-e^+\to\gamma\gamma} &\sim \xi^{4(2)} \left(\tfrac{m}{E}\right)^2 \left(\ln \tfrac{E}{m}\right)^4 \times 10^{-34}\mathrm{m}^2, \qquad E \gg m. \end{aligned} \tag{14}$$

In both cases in (14) the low and high energy limit are considered but the last one is more important here because there is a parameters space still unexplored. For example in LHC can be produced –probably as secondary photons– with 1 TeV of energy, then if $\omega \sim 1$ TeV could be possible cross sections comparable to the neutrino scattering ones [13], however this last fact needs a more detailed analysis.

This work was supported by FONDECYT/Chile grants 1130020 (J.G.), N.T. thanks to the Conicyt fellowship 21160064 and USA-1555 (A.A.). We would like to thank Prof. F. Méndez for useful discussions and Prof. S. L. Adler by suggesting us the reference [12].

[1] A. A. Abdo et al. (The Fermi LAT), Phys. Rev. Lett. **102**, 181101 (2009), 0905.0025.
[2] D. N. et . al, (WMAP), Astrophys. J. Suppl. **170**, 377 (207).
[3] M. Aguilar et al. (HEAT), Astrophys. J. **482**, L191 (1997).
[4] S. Torii et. al. (PPB-BETS) (2008), 0809.0760.
[5] O. Adriani (PAMELA), Nature **458**, 607 (2009).
[6] J. Chang, Nature **456**, 362 (2008).
[7] D. N. Spergel and P. J. Steinhardt, Phys. Rev. Lett. **84** (2000) 3760.
[8] N. Arkani-Hamed, D. P. Finkbeiner, T. R. Slatyer and N. Weiner, Phys. Rev. D **79** (2009) 015014.
[9] G. Breit and J. A. Wheeler,Phys. Rev. **46**, 1087 (1934).
[10] O. J. Pike, F. Mackenroth, E. G. Hill and S. J. Rose, Nature Photon. **8** (2014) 434.
[11] B. Holdom, Phys. Lett. B **166**, 196 (1986).
[12] R. Karplus and M. Neuman, Phys. Rev. **83**, 776 (1951).
[13] K. A. Olive et al. (Particle Data Group), Chin. Phys. C38, 090001 (2014).

[14] For a review see, J. Alexander *et al.*, arXiv:1608.08632 [hep-ph].

Physics Letters B 791 (2019) 17–19

Contents lists available at ScienceDirect

Physics Letters B

www.elsevier.com/locate/physletb

Anapole dark matter interactions as soft hidden photons

Paola Arias, J. Gamboa *, Natalia Tapia

Departamento de Física, Universidad de Santiago de Chile, Casilla 307, Santiago, Chile

ARTICLE INFO

Article history:
Received 14 January 2019
Received in revised form 13 February 2019
Accepted 16 February 2019
Available online 19 February 2019
Editor: J. Hisano

Keywords:
Dark matter
Hidden photons

ABSTRACT

We propose a model where the anapole appears as a hidden photon that is coupled to visible matter through a kinetic mixing. For low momentum $|\mathbf{p}| \ll M$ where M is the cutoff the model (soft hidden photon limit) is reduced to the Ho-Scherrer description. We show that the hidden gauge boson is stable and therefore hidden photons are indeed, candidates for dark matter. Our approach shows that anapole and kinetic mixing terms are equivalent descriptions seen from different scales of energy.

Majorana fermions are particles that feature good attributes to be considered dark matter [1] candidates. On the one hand they are electrically neutral and can interact with virtual photons. However, there are several ways to implement the dark matter idea as, for example, by including neutralinos [2], analyzing relic abundance systematically [3], incorporating Sommerfeld enhancement [4,5] or extending the standard model through the use of secret interactions [6], kinetic mixing [8] and so on.

However there are also other reasons that justify an additional study of Majorana fermions as dark matter, namely, it is expected that the effects of dark matter will be more accessible in the low energy sector, and if the dark matter is coupled with the standard model, then effects such as parity violation can play an important role [9].

As in any effective theory one expects that there is a cut-off energy M, for which if $E \simeq M$, both the parity violation and the anapole contributions provide visible signals as a consequence, most likely, of more fundamental symmetries unknown until now.

The consequences of the description above are followed by the fact that the vertex function $\Gamma^{\mu}(q^2)$ must be consistent with gauge invariance because it is related to the electromagnetic current through

$$\langle k|J^{\mu}|k'\rangle = \bar{u}(\mathbf{k})\Gamma^{\mu}(q^2)u(\mathbf{k}'),$$

where $\Gamma^{\mu}(q^2)$ has the following general structure

$$\Gamma^{\mu} = F_1(q^2)\gamma^{\mu} + F_2(q^2)\frac{i}{2\bar{m}}\sigma^{\mu\nu}p_{\nu} + F_3(q^2)\frac{i}{2m}\sigma^{\mu\nu}q_{\nu}\gamma_5 + F_4(q^2)(\gamma^{\mu}q^2 - q^{\mu}\not{q})\gamma_5, \tag{1}$$

where the $F_{1,2,3,4}$ are form factors and $q^2 = -(k-k')^2$.

The term proportional to F_3 is the electric dipole moment which violates temporal inversion but is invariant under parity, while the term proportional to F_4 is called the anapole contribution [10] and violates both parity and temporal inversion.

The Lagrangian that provides the anapole contribution is [11,12]

$$\mathcal{L}_{\text{anapole}} = -\frac{g}{M^2}\bar{\chi}\gamma_{\mu}\gamma_5\chi\ \partial_{\nu}F^{\mu\nu}, \tag{2}$$

where $F_{\mu\nu} = \partial_{\mu}A_{\nu} - \partial_{\nu}A_{\mu}$ is the strength tensor, g is a dimensionless coupling constant and M is a cutoff of mass.

In a more classical context, and inspired by the remarkable ideas developed in the late fifties in weak interactions physics [13], the hypothesis of identifying Majorana fermions with dark matter is even more intriguing because the electromagnetic interaction [10] with Majorana fermions should occur through the anapole term [11,12].

Intuitively, the anapole interaction appears when neutral fermions are coupled through the process shown in Fig. 1, where the black box vertex encodes the parity violation [10]. Then, the possible relation between dark matter and fermions of the standard model (f) emerges when we "paste" the processes $\chi\bar{\chi} \to \gamma$

* Corresponding author.
E-mail addresses: paola.arias.r@usach.cl (P. Arias), jorge.gamboa@usach.cl (J. Gamboa), natalia.tapiaa@usach.cl (N. Tapia).

https://doi.org/10.1016/j.physletb.2019.02.021

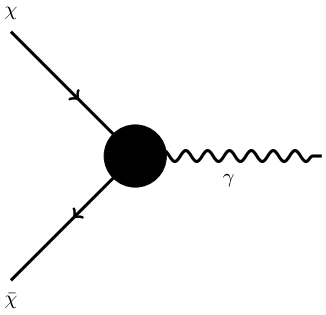

Fig. 1. Annihilation of two Majorana fermions into a virtual photon. The black box is an effective vertex.

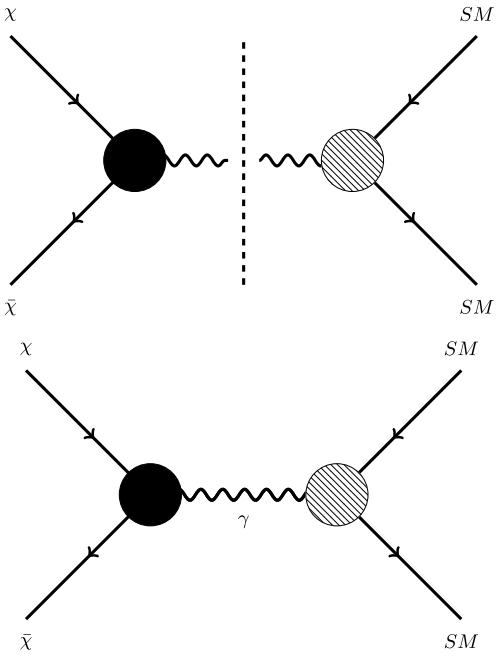

Fig. 2. This diagram 'pastes' the dark (LHS) and visible (RHS) parts through a virtual photon.

and $\gamma \to \bar{f} f$, with γ a virtual photon playing the role of a "bridge" between dark matter and the standard model (see Fig. 2).

The goal of this paper is to present an approach that shows a very clear relationship between hidden photons and anapole as dark matter. In a nutshell, our results show that the anapole term can emerge from a soft hidden photon limit approximation.

An extra U(1) gauge boson - often referred as hidden photon or dark photon - it is a quite interesting and well motivated dark matter candidate. Has been pointed out that such particle can explain the whole dark matter content observed today, or be a subdominant component, if produced a non-thermally during inflation [14].

In order to explain the idea we begin considering the Lagrangian

$$\mathcal{L} = \mathcal{L}(\{\chi, G_\mu\}, \{\psi, G_\mu\}), \tag{3}$$

where $\{\chi, G_\mu\}$ correspond to the particle content of the dark sector, with G_μ a hidden $U(1)$ gauge field, whereas in $\{\psi, A_\mu\}$ the ψ's are fermions of the standard model and A_μ is the visible photon.

More specifically (3) will be written as

$$\mathcal{L} = \bar{\chi}\left(i\partial\!\!\!/ - g\gamma_5 G\!\!\!/ - \bar{m}\right)\chi - \frac{1}{4}G^2_{\mu\nu}(G) + \frac{1}{2}M^2 {G_\mu}^2 + \bar{\psi}\left(i\partial\!\!\!/ - gA\!\!\!/ - m\right)\psi - \frac{1}{4}F^2_{\mu\nu}(A) + \frac{\xi}{2}F_{\mu\nu}(A)G^{\mu\nu}(G) + \cdots, \tag{4}$$

with the strength tensors $F_{\mu\nu}(A)$ and $G_{\mu\nu}(G)$ defined as

$$F_{\mu\nu}(A) = \partial_\mu A_\nu - \partial_\nu A_\mu,$$
$$G_{\mu\nu}(G) = \partial_\mu G_\nu - \partial_\nu G_\mu. \tag{5}$$

In (4), ξ parametrizes the (small) kinetic mixing between hidden and visible photons, and $\cdots$ denotes all other fields belonging to the standard model.

A mass term, M, for the hidden photon has been included, assuming that there is a particular spontaneous symmetry breaking mechanism in the hidden sector or corresponds to a stueckelberg mass term (see also [7]).

The next step is to consider a region in which the hidden photon momentum satisfies $|\mathbf{p}| \ll M$, such limit can be justified for a hidden photon dark matter candidate, since $|\mathbf{v}_{dm}| \ll 1$, so that in this limit the kinetic term $G^2_{\mu\nu}$, is much smaller than $M^2 G^2_\mu$, so

$$\mathcal{L} = \bar{\chi}\left(i\partial\!\!\!/ - g\gamma_5 G\!\!\!/ - \bar{m}\right)\chi + \frac{1}{2}M^2 {G_\mu}^2 + \bar{\psi}\left(i\partial\!\!\!/ - gA\!\!\!/ - m\right)\psi - \frac{1}{4}F^2_{\mu\nu}(A) - \xi G_\nu \partial_\mu F^{\mu\nu}(A) + \cdots. \tag{6}$$

Where we have made an integration by parts of the kinetic mixing term.

In this region of energy, G_μ becomes an auxiliary field, and therefore can be found to be

$$G_\mu = \frac{1}{M^2}\left(g\bar{\chi}\gamma_\mu\gamma_5\chi + \xi\partial^\nu F_{\mu\nu}(A)\right).$$
$$= \frac{1}{M^2}\left(g J^{(5)}_\mu + \xi\partial^\nu F_{\mu\nu}(A)\right). \tag{7}$$

Putting back the latter expression for G_μ into (6) we get

$$\mathcal{L} \simeq \bar{\chi}\left(i\partial\!\!\!/ - \bar{m}\right)\chi - \frac{g^2}{M^2}\left(\bar{\chi}\gamma_\mu\gamma_5\chi\right)^2 - \xi\frac{g}{M^2}\bar{\chi}\gamma_\mu\gamma_5\chi\ \partial_\nu F^{\mu\nu} + \mathcal{O}(\xi^2). \tag{8}$$

Thus, from the above equation can be clearly seen that the anapole term comes from the "soft-photons" approximation, meaning from the assumption that the momentum of the hidden photon is much smaller than M.

However, we also emphasize that the anapole contribution is a consequence of the kinetic mixing of the dark matter as it becomes explicit by the presence of ξ. Therefore, a Majorana fermion coupled to the DM particle can manifest itself via an anapole interaction.

The measurement of anapole contributions is a task that has been developing slowly, where these contributions are considered a test of precision of the standard model. Currently there are several experiments running in atomic physics [15], that complement the first measurement in this direction [16].

In the context of anapole contributions coming from dark matter, these are more difficult to control and what we have proposed in this letter is to address them via kinetic mixing.

The point of view considered here unifies two apparently different approaches and allows to establish a one-to-one correspondence between both.

Another interesting question is to investigate the stability of the G_μ boson. In the static limit this boson is, of course, stable but if G_μ is a dynamical field, then one should worry about its life time.

In order to do so, it is convenient to take the basis (A_μ, G_μ) and diagonalize it, so the mass eigenstates will be

$$A_\mu \cong A'_\mu + g\left(1+\frac{m^2}{M^2}\right)G'_\mu$$
$$G_\mu \cong A'_\mu - g\frac{m^2}{M^2}G'_\mu \tag{9}$$

And the Lagrangian in the hidden sector becomes

$$\mathcal{L} \subset -g^2\frac{m^2}{M^2}G'_\mu\bar{\chi}\gamma_5\gamma^\mu\chi,$$

so the decay with is given by [17]

$$\Gamma(G\to\bar{\chi}\chi) \cong g^2\left(\frac{m}{M}\right)^4 m. \tag{10}$$

However, as in many extensions of the standard model, it is sensible to consider $m \ll M$, thus, the decay amplitude it is indeed small, implying that the average life time of the gauge boson is large, at least compared to the life time of the universe, so the boson G_μ is stable.

From the point of view of the phenomenological possibilities of detection one could explore at least two; the first one requires an exhaustive analysis of the data XENON100 [18], and the second is to exploit the extra Coulomb contribution that results from the Lagrangian of eq. (6), namely [15]

$$V(r) = \frac{g}{4\pi}\frac{e^{-Mr}}{r}\gamma_5,$$

which is the lowest order contribution.

Classical experiments of Coulomb's law, bounds on the photon mass [19] and parity violation tests could, in principle, provide some clues about the existence of dark matter in the universe.

We would like to thank Prof. F. Mendez and F.A. Schaposnik by discussions. This work was supported DICYT (J.G.) and FONDECYT-Chile project 1161150 (P.A.), and CONICYT Fellowship 21160064 (N.T.).

References

[1] G. Bertone, D. Hooper, J. Silk, Phys. Rep. 405 (2005) 279;
K. Petraki, R.R. Volkas, Int. J. Mod. Phys. A 28 (2013) 1330028;
A. Kusenko, Phys. Rep. 481 (2009) 1;
J. Hisano, S. Matsumoto, M. Nagai, O. Saito, M. Senami, Phys. Lett. B 646 (2007) 34.
[2] L. Bergstrom, P. Ullio, J.H. Buckley, Astropart. Phys. 9 (1998) 137;
E.A. Baltz, J. Edsjo, K. Freese, P. Gondolo, Phys. Rev. D 65 (2002) 063511;
G. Jungman, M. Kamionkowski, K. Griest, Phys. Rep. 267 (1996) 195.
[3] P. Agrawal, N. Kitajima, M. Reece, T. Sekiguchi, F. Takahashi, arXiv:1810.07188 [hep-ph];
H. Iminniyaz, M. Drees, X. Chen, J. Cosmol. Astropart. Phys. 1107 (2011) 003.
[4] N. Arkani-Hamed, D.P. Finkbeiner, T.R. Slatyer, N. Weiner, Phys. Rev. D 79 (2009) 015014;
J.L. Feng, Annu. Rev. Astron. Astrophys. 48 (2010) 495.
[5] J. Jaeckel, A. Ringwald, Annu. Rev. Nucl. Part. Sci. 60 (2010) 405;
R. Essig, et al., arXiv:1311.0029 [hep-ph];
S. Tulin, H.B. Yu, Phys. Rep. 730 (2018) 1.
[6] K.C.Y. Ng, J.F. Beacom, Phys. Rev. D 90 (6) (2014) 065035;
K.C.Y. Ng, J.F. Beacom, Phys. Rev. D 90 (8) (2014) 089904, Erratum;
F. Forastieri, M. Lattanzi, P. Natoli, J. Cosmol. Astropart. Phys. 1507 (07) (2015) 014;
M.S. Bilenky, A. Santamaria, arXiv:hep-ph/9908272;
D. Carcamo, J. Gamboa, F. Mendez, A.K. Das, A.P. Polychronakos, Phys. Rev. D 91 (2015) 065028.
[7] F. Englert, R. Brout, Phys. Rev. Lett. 13 (1964) 321.
[8] B. Holdom, Phys. Lett. B 166 (1986) 196.
[9] A. Lue, L.M. Wang, M. Kamionkowski, Phys. Rev. Lett. 83 (1999) 1506.
[10] Y.B. Zeldovich, J. Exp. Theor. Phys. 33 (1958) 1184.
[11] C.M. Ho, R.J. Scherrer, Phys. Lett. B 722 (2013) 341;
Y. Gao, C.M. Ho, R.J. Scherrer, Phys. Rev. D 89 (4) (2014) 045006.
[12] D.C. Latimer, Phys. Rev. D 95 (9) (2017) 095023;
S. Kang, S. Scopel, G. Tomar, J.H. Yoon, P. Gondolo, arXiv:1808.04112 [hep-ph];
A. Alves, A.C.O. Santos, K. Sinha, Phys. Rev. D 97 (5) (2018) 055023;
X. Chu, J. Pradler, L. Semmelrock, arXiv:1811.04095 [hep-ph].
[13] T.D. Lee, C.N. Yang, Phys. Rev. 104 (1956) 254.
[14] P.W. Graham, J. Mardon, S. Rajendran, Phys. Rev. D 93 (10) (2016) 103520, https://doi.org/10.1103/PhysRevD.93.103520, arXiv:1504.02102 [hep-ph].
[15] M.S. Safronova, D. Budker, D. DeMille, D.F.J. Kimball, A. Derevianko, C.W. Clark, Rev. Mod. Phys. 90 (2) (2018) 025008.
[16] C.S. Wood, S.C. Bennett, D. Cho, B.P. Masterson, J.L. Roberts, C.E. Tanner, C.E. Wieman, Science 275 (1997) 1759.
[17] C.R. Chen, F. Takahashi, T.T. Yanagida, Phys. Lett. B 673 (2009) 255;
C.R. Chen, F. Takahashi, T.T. Yanagida, Phys. Lett. B 671 (2009) 71.
[18] J. Angle, et al., XENON Collaboration, Phys. Rev. Lett. 100 (2008) 021303.
[19] M. Tanabashi, et al., Particle Data Group, Phys. Rev. D 98 (3) (2018) 030001.